

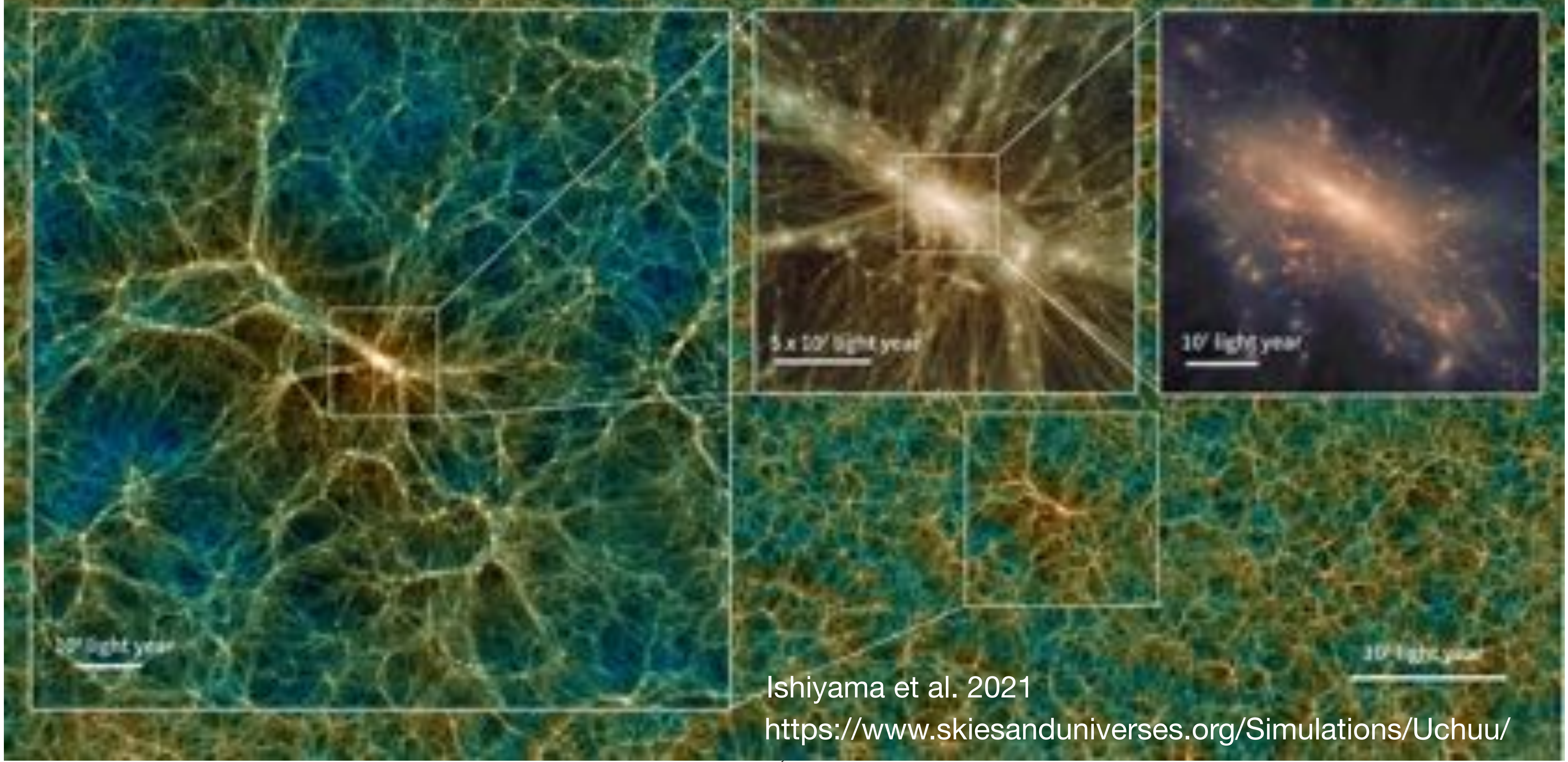
Modelling the clustering and halo occupation of DESI tracers with Uchuu

by Francisco Prada

Instituto de Astrofísica de Andalucía CSIC

Granada, Spain

| Simulation Name | Lbox Mpc/h | Npart | Mpart Msun/h |
|-----------------|---------------|--------------------|-----------------|
| Uchuu | 2000 | 12800 ³ | 3.27e8 |



Ishiyama et al. 2021

<https://www.skiesanduniverses.org/Simulations/Uchuu/>

Uchuu lightcone mocks for DESI 1%

A. Production Steps:

1. Generating DESI galaxies and QSOs using SHAM methods for tracer-halo connections using V_{peak} with scatter,
2. Creating Uchuu full-sky lightcones by concatenating boxes at several redshifts,
3. Running the LSS pipeline on the Uchuu lightcones to measure the clustering signal,
4. Verifying that the Uchuu lightcones reproduce the observed evolution of clustering with redshift and the clustering dependence on tracer global properties.

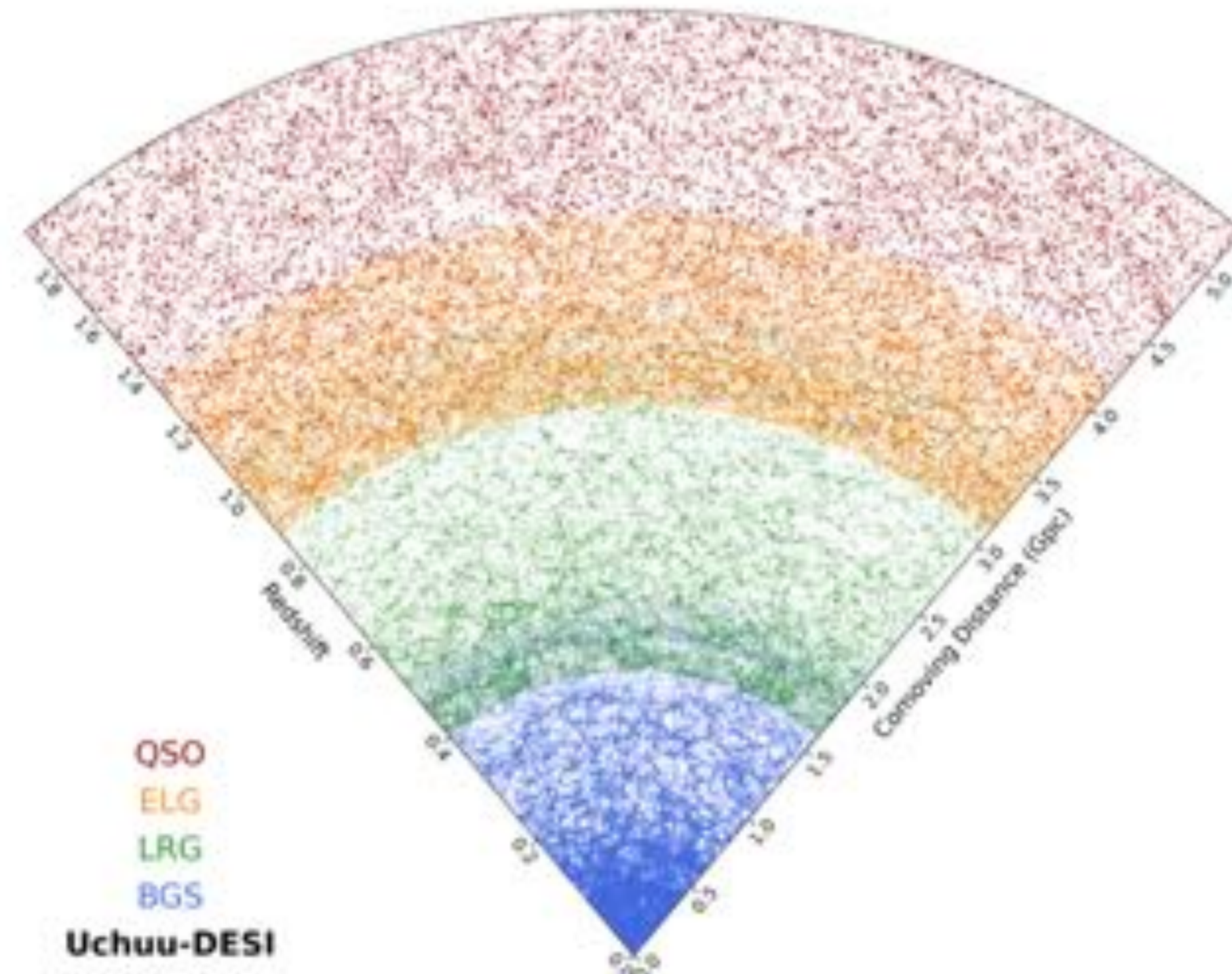
B. Data Catalog:

['RA', 'DEC', 'Z', 'Z_noRSD', 'PID', 'B1', 'Unique_id', 'Tracer_type', WEIGHT]

'PID' = -1 (distinct halo) or 0 (subhalo)

'B1' is a baryonic property

Prada et al. 2025 for DESI 1% (arXiv:2306.06315)



DESI 1% Sky Footprint

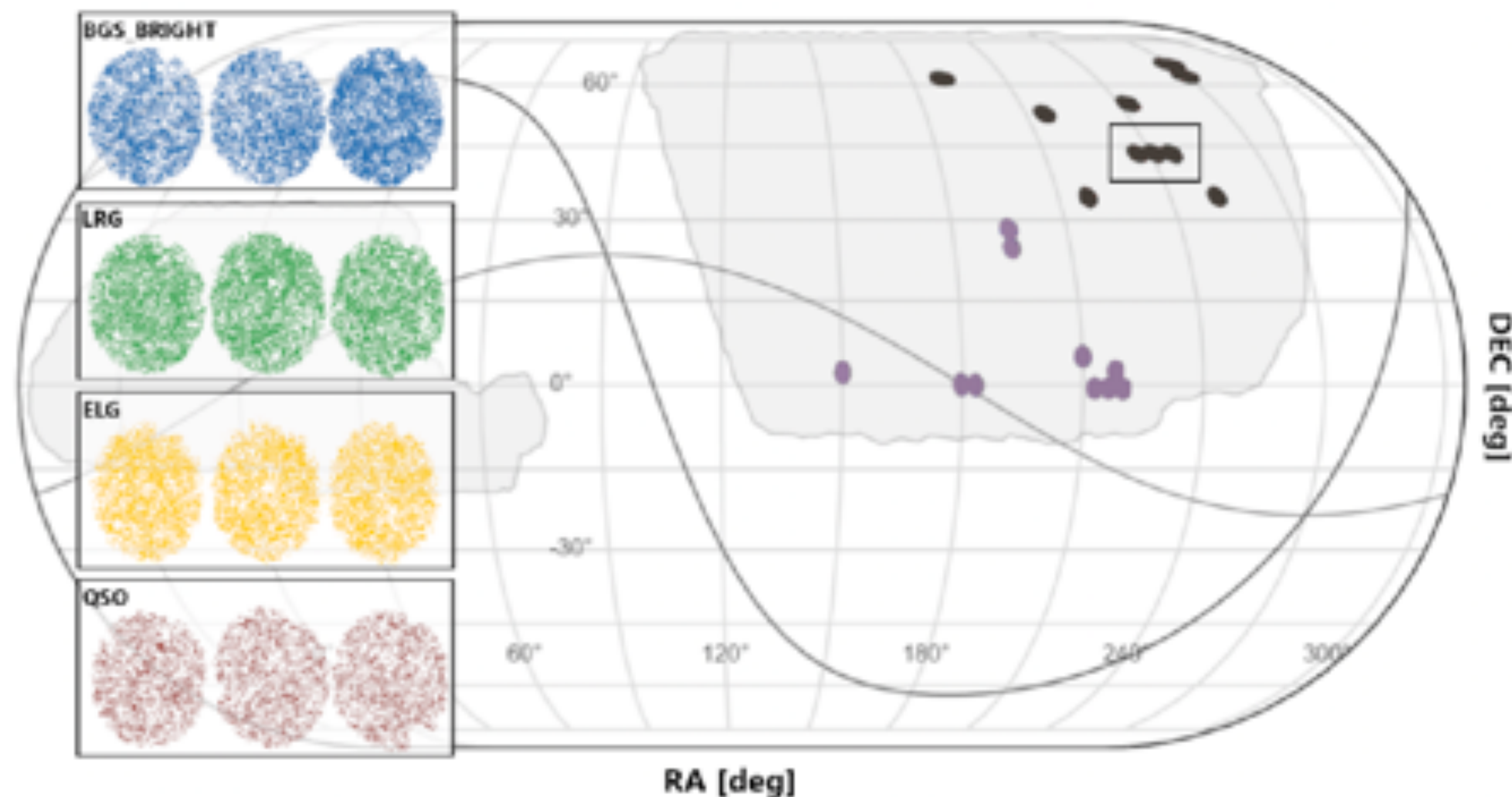


Table 1. Basic properties of the DESI One-Percent Survey samples used in this work.

| Sample | Redshift range | z_{med} | A_{eff} (deg ²) | N_{eff} | $10^2 \times V_{\text{eff}}$ ($h^{-3} \text{Gpc}^3$) |
|------------|-------------------|------------------|---|------------------|---|
| BGS-BRIGHT | $0.05 < z < 0.5$ | 0.21 | 173.5 | 142341 | 3.72 |
| LRG | $0.45 < z < 0.85$ | 0.76 | 166.9 | 58764 | 7.97 |
| ELG | $0.88 < z < 1.34$ | 1.07 | 168.6 | 156891 | 12.95 |
| QSO | $0.9 < z < 2.1$ | 1.53 | 174.6 | 23085 | 1.87 |

Notes. The redshift interval, median redshift (z_{med}), effective area of the sky footprint weighted by completeness (A_{eff}), number of galaxies (N_{eff}), and effective volume (V_{eff}).

Fig. 1. Sky coverage of the DESI One-Percent Survey for the BGS-BRIGHT, LRG, ELG, and QSO cosmological tracers used in this analysis. The 20 rosettes that make up the One-Percent footprint are split into 'north' (in black) and 'south' (in purple). The grey-shaded regions indicate the expected DESI Year-5 sky coverage. The four small panels are zoomed in on a section of the footprint covered by 3 rosettes, for each tracer. The colour-coding represents the angular weighted number density, where darker colours indicate a higher density.

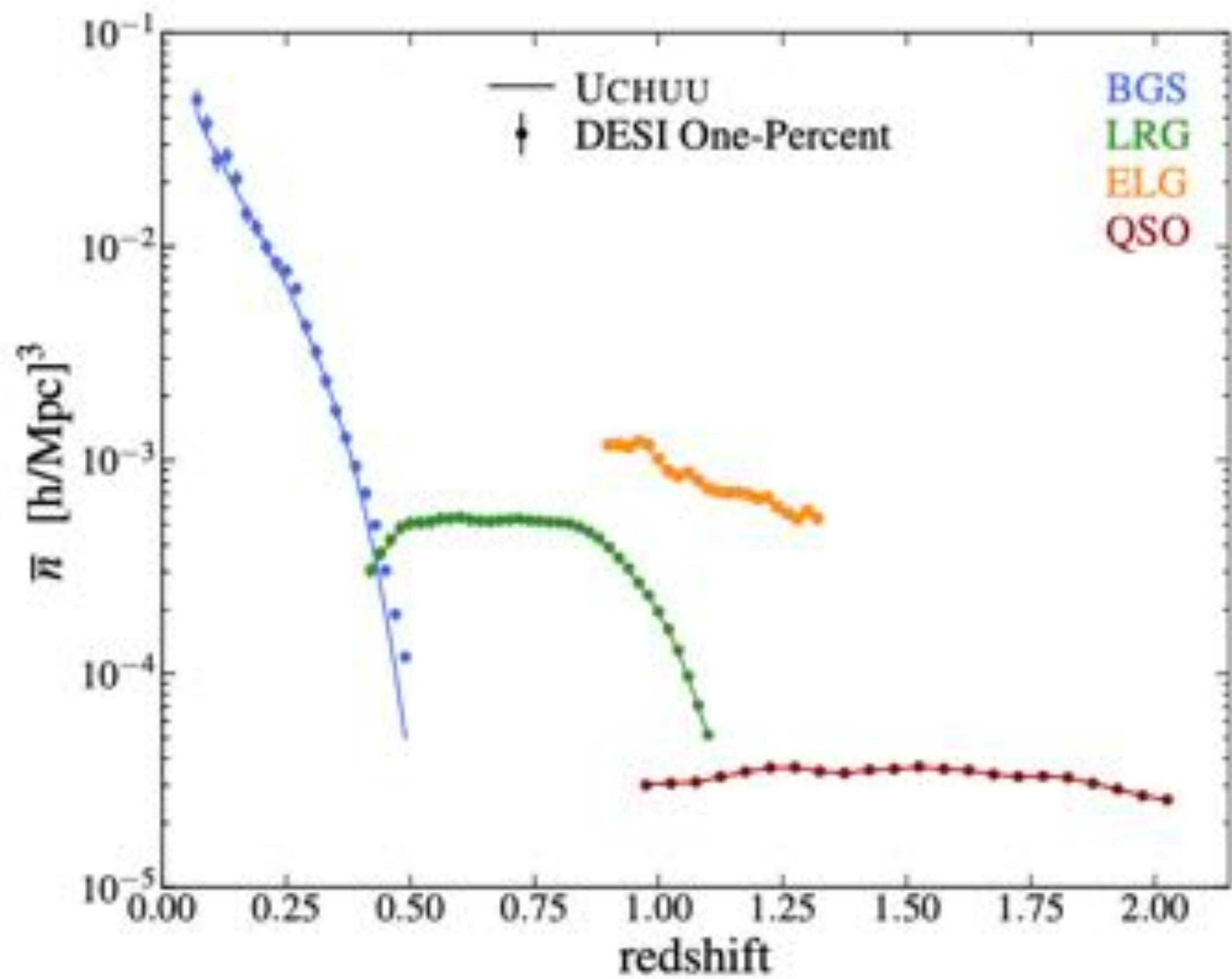


Fig. 2. Comoving number density of the four DESI One-Percent tracer samples (points) and the average of the corresponding UCHUU-DESI mock lightcones (solid line) over the entire redshift range $0.1 < z < 2.1$. Data error bars are obtained from the ensemble of UCHUU One-Percent lightcones built in this work.

Subhalo Abundance Matching (SHAM)

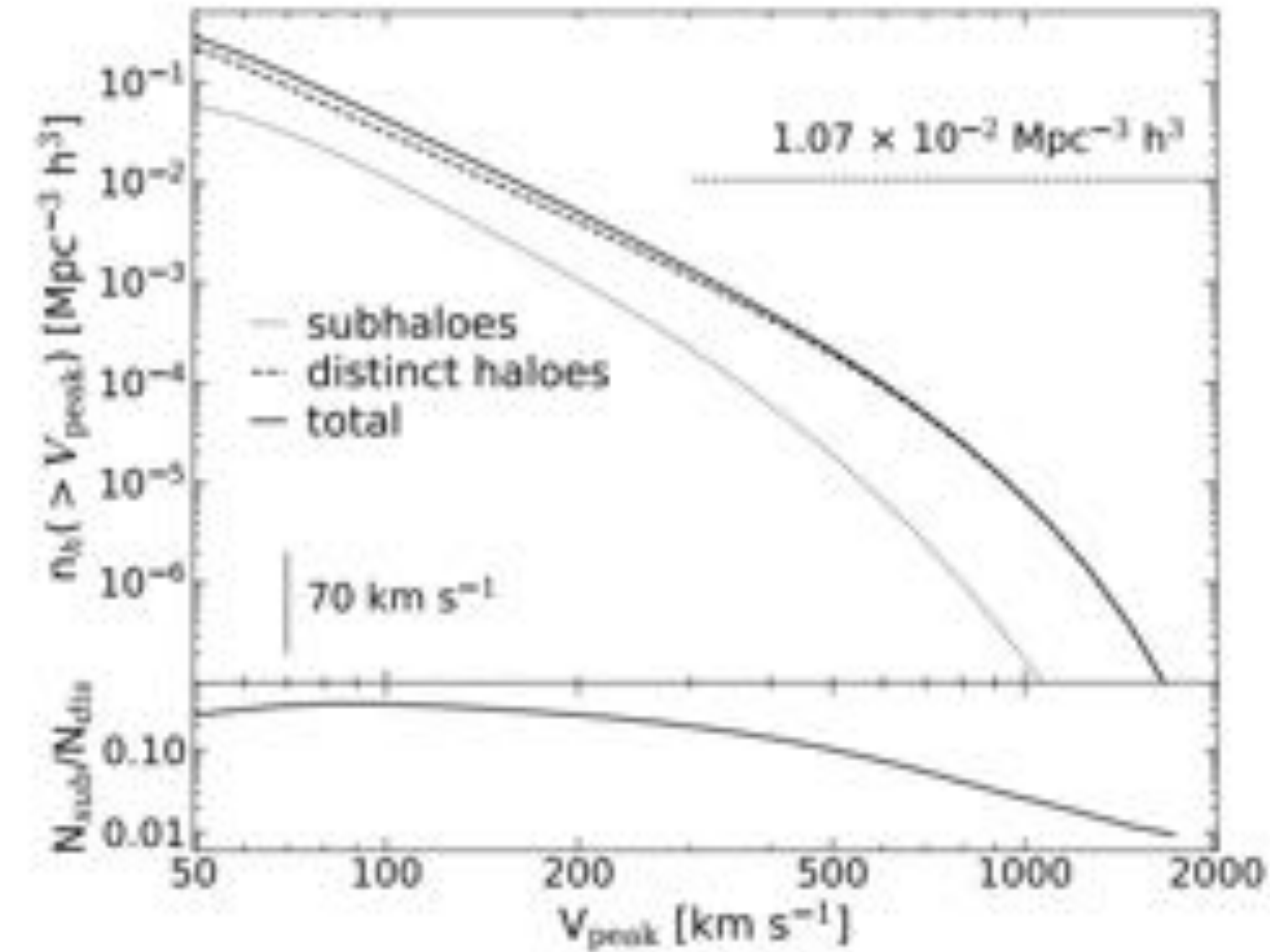


Fig. 3. Top panel: Cumulative number density of distinct haloes (N_{dist}) (dashed curve), subhaloes (N_{sub}) (dotted curve), and all haloes (solid curve) as a function V_{peak} in the UCHUU simulation box at $z = 0.2$, the median redshift of the BGS-BRIGHT sample in the DESI One-Percent Survey. The horizontal line indicates the mean number density of the BGS-BRIGHT sample. The vertical line indicates the completeness threshold for UCHUU. Bottom panel: Cumulative subhalo fraction measured as a function of V_{peak} .

The basic assumption of the Subhalo Abundance Matching (SHAM) method is that massive haloes host massive galaxies. This allows one to generate a rank-ordered relation between dark matter haloes and galaxies. However, observations show that this assignment cannot be a one-to-one relation. In order to create a more realistic approach, it is necessary to include scatter in this matching. SHAM relates galaxy luminosities or stellar mass from galaxies to a halo property. We use the peak value of the circular velocity over the history of the halo (V_{peak}), which has advantages compared to the halo mass (M_{halo}). M_{halo} is well defined for host haloes, but its definition becomes ambiguous for subhaloes.

$$n_{\text{gal}}(> M_*^i) = n_{\text{halo}}(> V_{\text{peak},i}^{\text{scat}}).$$

This relation implies that a halo with $V_{\text{peak},i}^{\text{scat}}$ will contain a galaxy with stellar mass M_*^i .

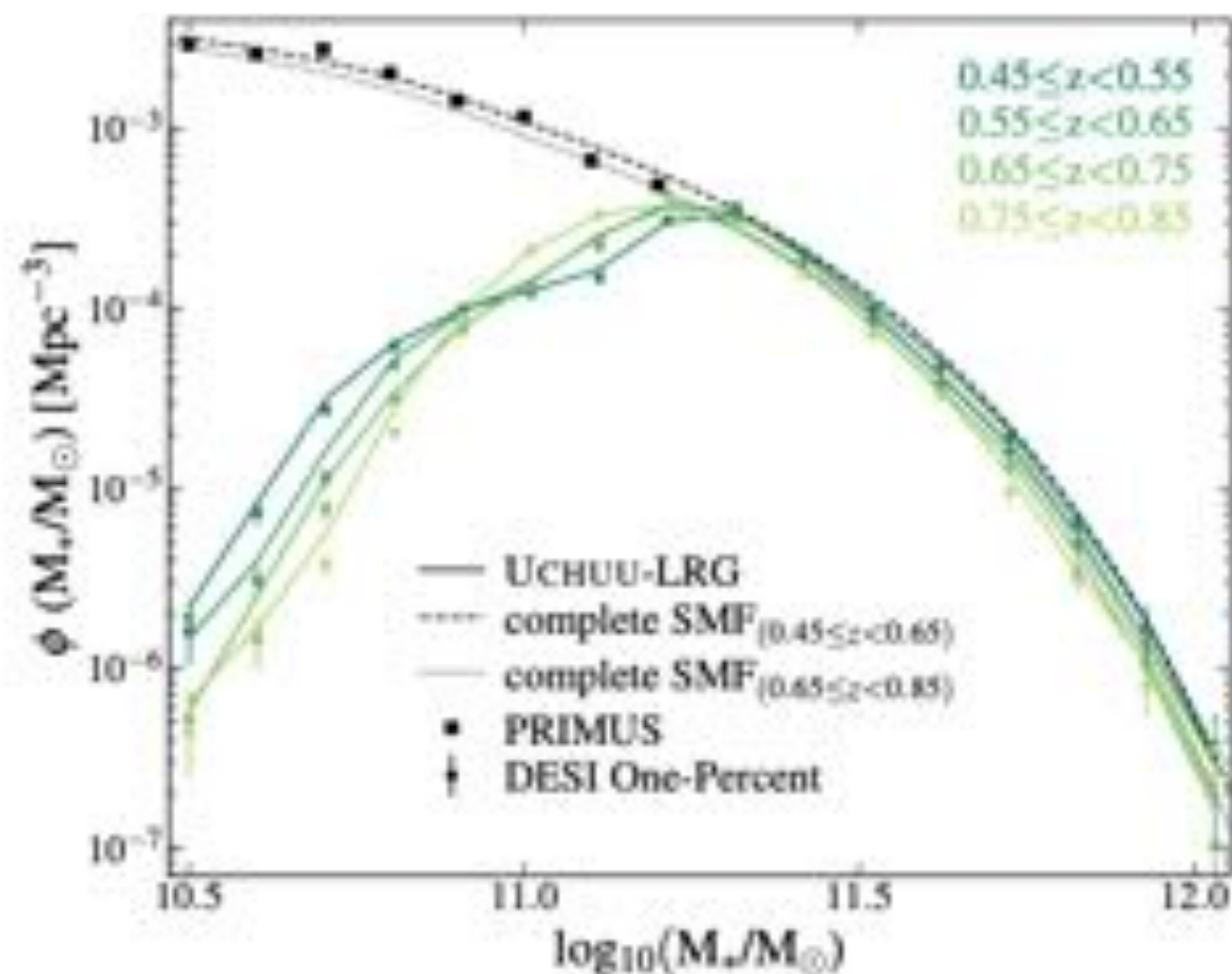


Fig. 4. Stellar mass functions for LRG in the DESI One-Percent Survey (points) and the mean of our UCHUU-LRG lightcones (solid curves) are shown for several redshift bins within the range $0.45 < z < 0.85$. The dashed curves represent the complete SMF adopted in each redshift range, indicated in the legend. Data error bars and the model shaded area represent the standard deviation of our set of 102 UCHUU lightcones.

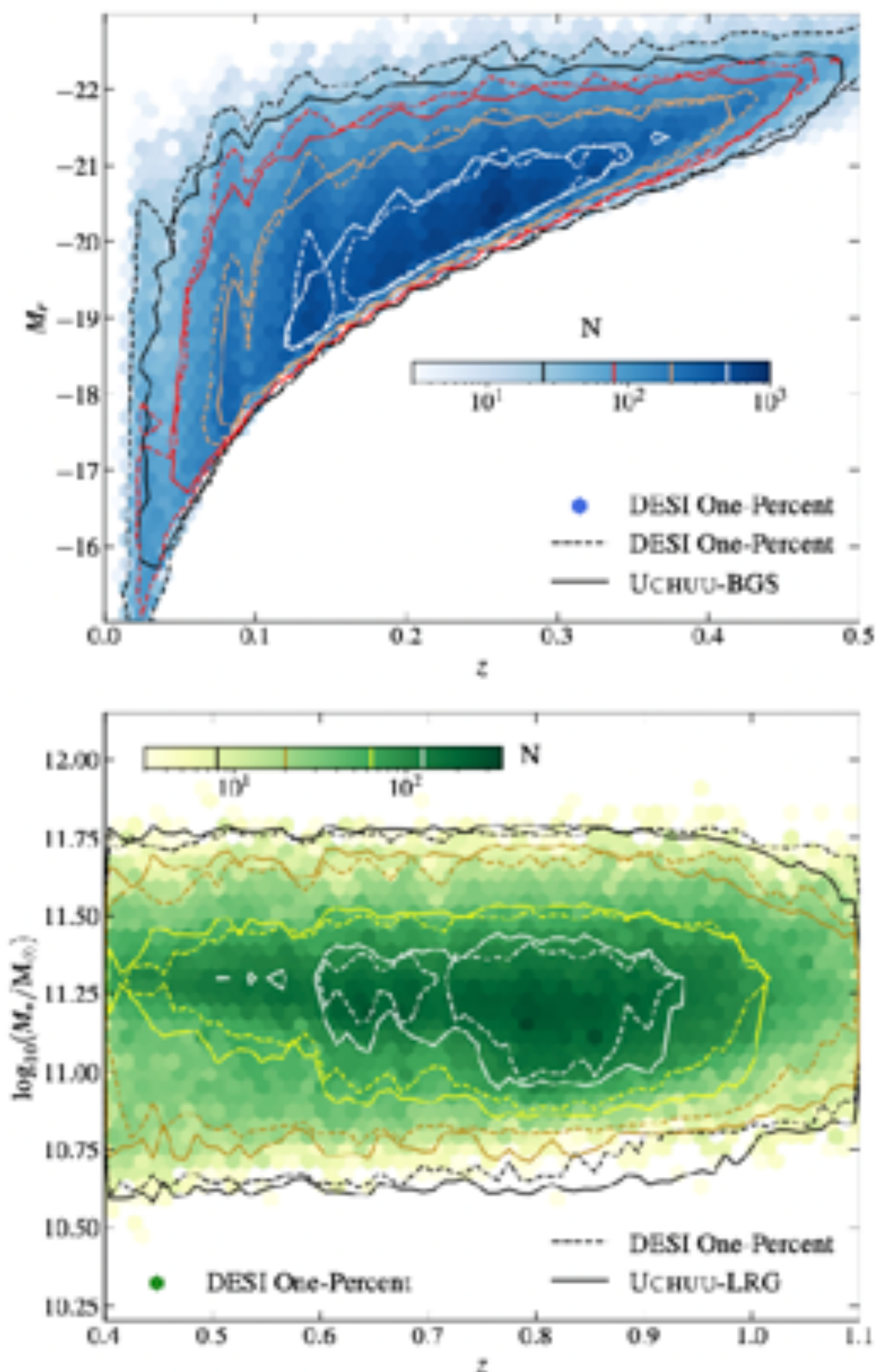
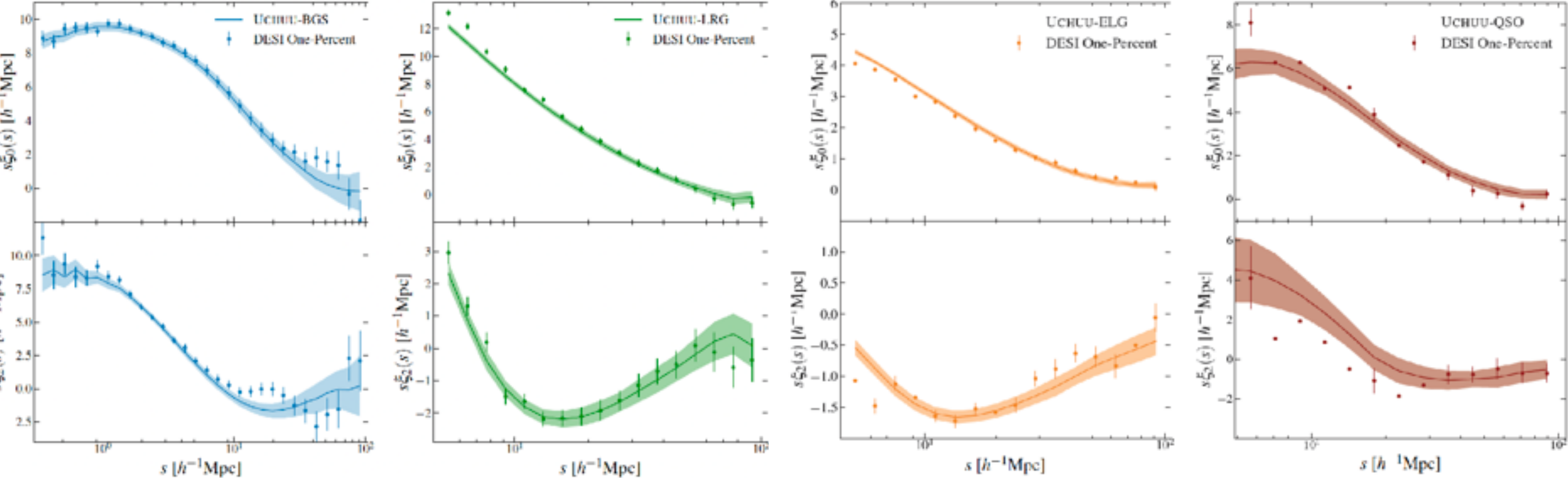


Fig. 6. Top panel: Absolute magnitude versus redshift for the DESI One-Percent BGS sample (hexagonal bins), compared to one of the UCHUU-BGS lightcones (contours). Absolute magnitudes have been k - and E -corrected. Bottom panel: Logarithm of the stellar mass vs. redshift for the DESI One-Percent LRG sample (hexagonal bins), compared to one of the UCHUU-LRG lightcones (contours).

Measurements of the monopole and quadrupole of the redshift-space correlation function for all four tracers from the DESI 1% samples, in the redshift intervals $0.1 < z < 0.3$ (BGS), $0.45 < z < 0.85$ (LRG), $0.88 < z < 1.34$ (ELG), and $0.9 < z < 2.1$ (QSO). The theoretical predictions from the mean of the independent Uchuu-DESI lightcones generated for each tracer are shown as solid curves, while the shaded areas correspond to the error from the RMS of the 102 mocks.



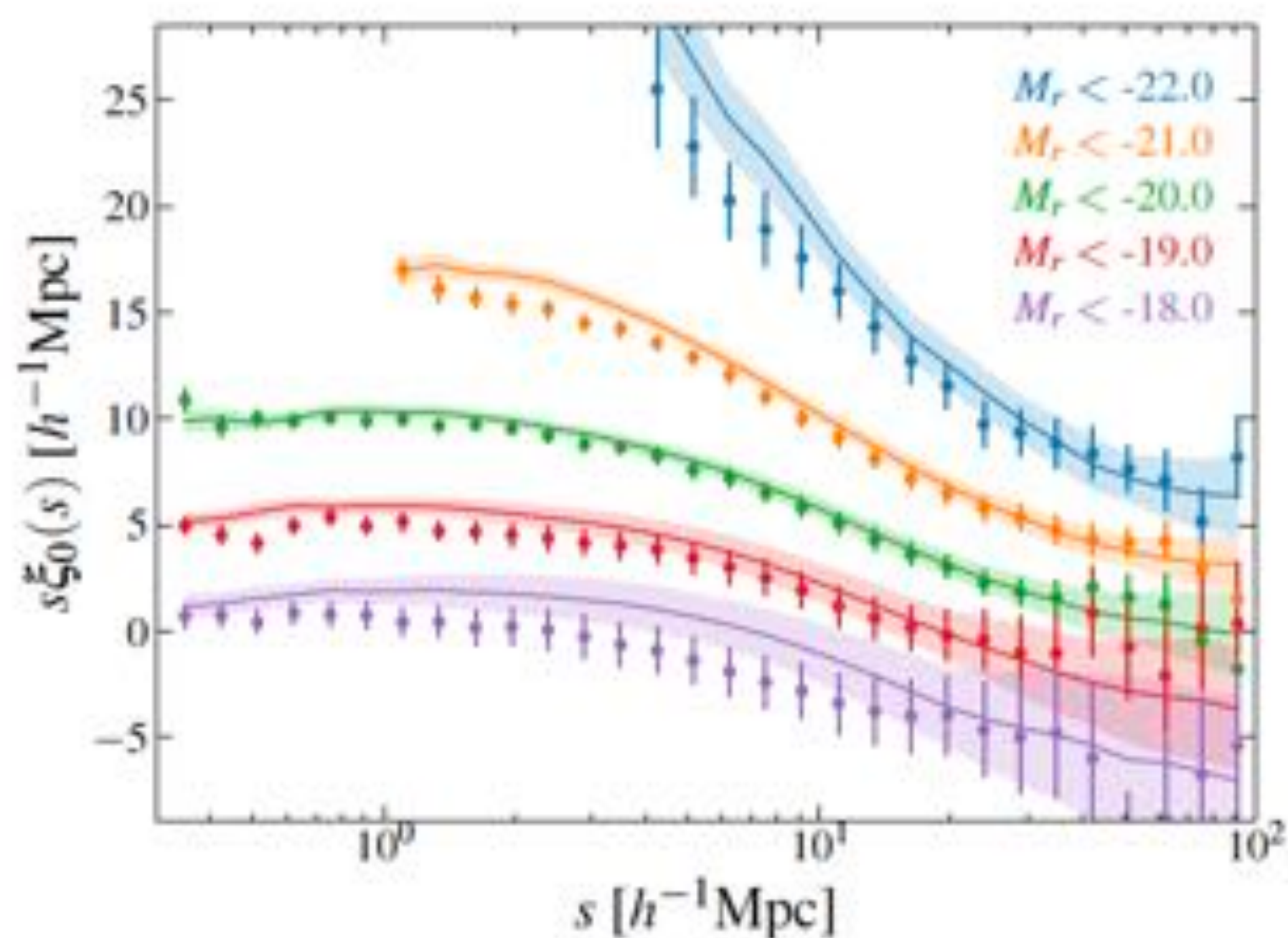


Fig. 8. Monopole of the correlation function for BGS galaxies in volume-limited samples. The legend shows different magnitude thresholds with corresponding colours. The solid curves represent the mean of 102 independent UCHUU One-Percent mocks, while the shaded region denotes the error from the RMS of the mocks. DESI One-Percent clustering measurements are indicated by the points with error bars, where the errors are the 1σ scatter between the mocks. Each magnitude threshold sample is vertically offset relative to the $M_r < -20$ sample.

Halo Occupation Distribution of Galaxies and QSO in the DESI 1% sample

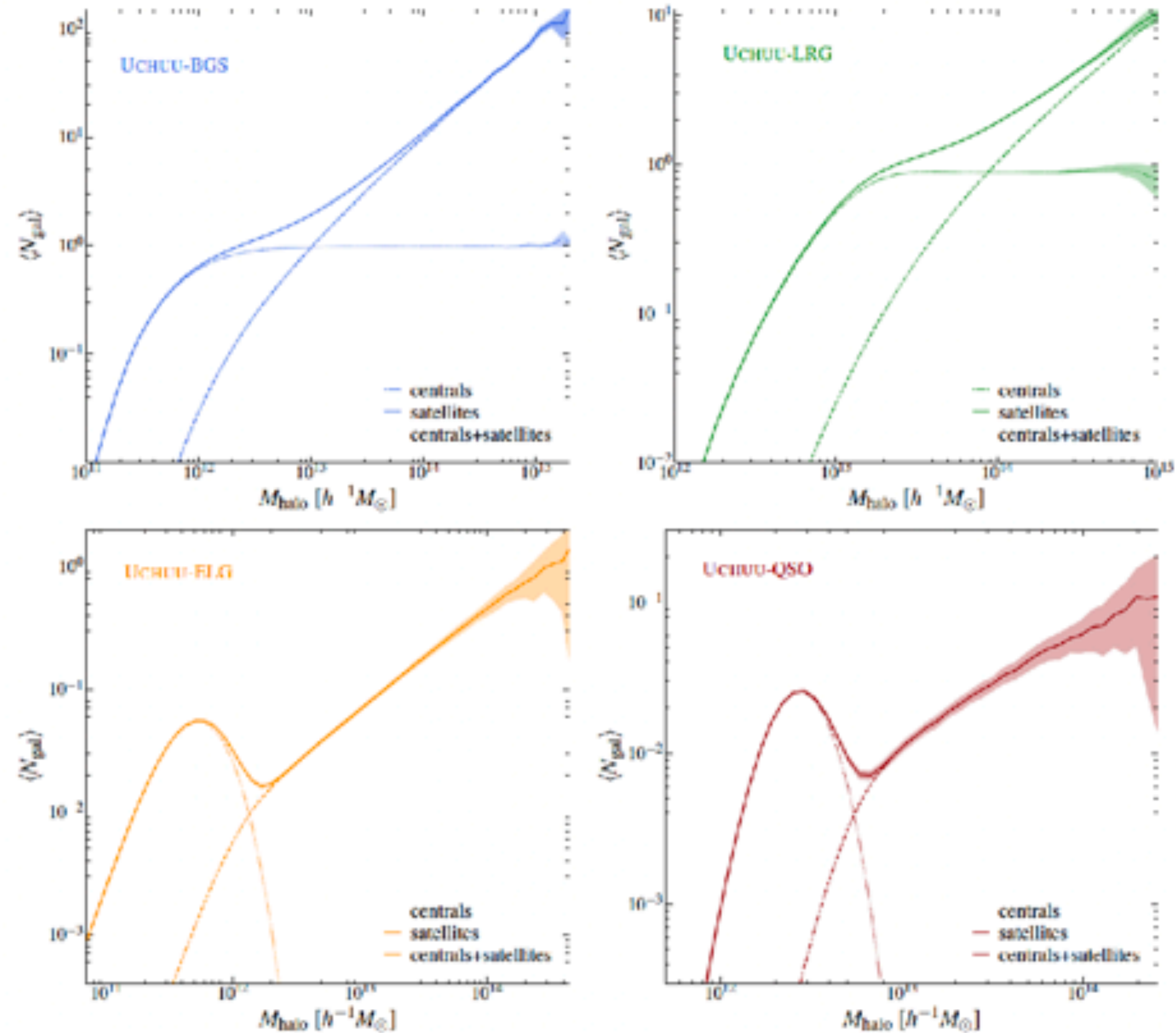


Fig. 13. Mean halo occupancy of BGS (top-left panel), LRG (top-right panel), ELG (bottom-left panel), and QSO (bottom-right panel) samples, as determined from our (modified) SHAM UCHUU lightcones. The mean number of galaxies of a halo with a given mass M_{halo} is denoted by $\langle N_{\text{gal}} \rangle$. The solid lines represent the combined centrals and satellite occupation, while the dotted and dashed lines show the mean halo occupancy for centrals and satellites, respectively. The shaded area indicates the 1σ uncertainty of the occupation measured from the UCHUU lightcones. For BGS, this is a jackknife error from the full-sky mock, split into 100 jackknife regions. For the other tracers, this is the 1σ scatter between the 102 mocks. The best-fit HOD model parameters for BGS and LRG are listed in Tables 4 and 5, respectively.

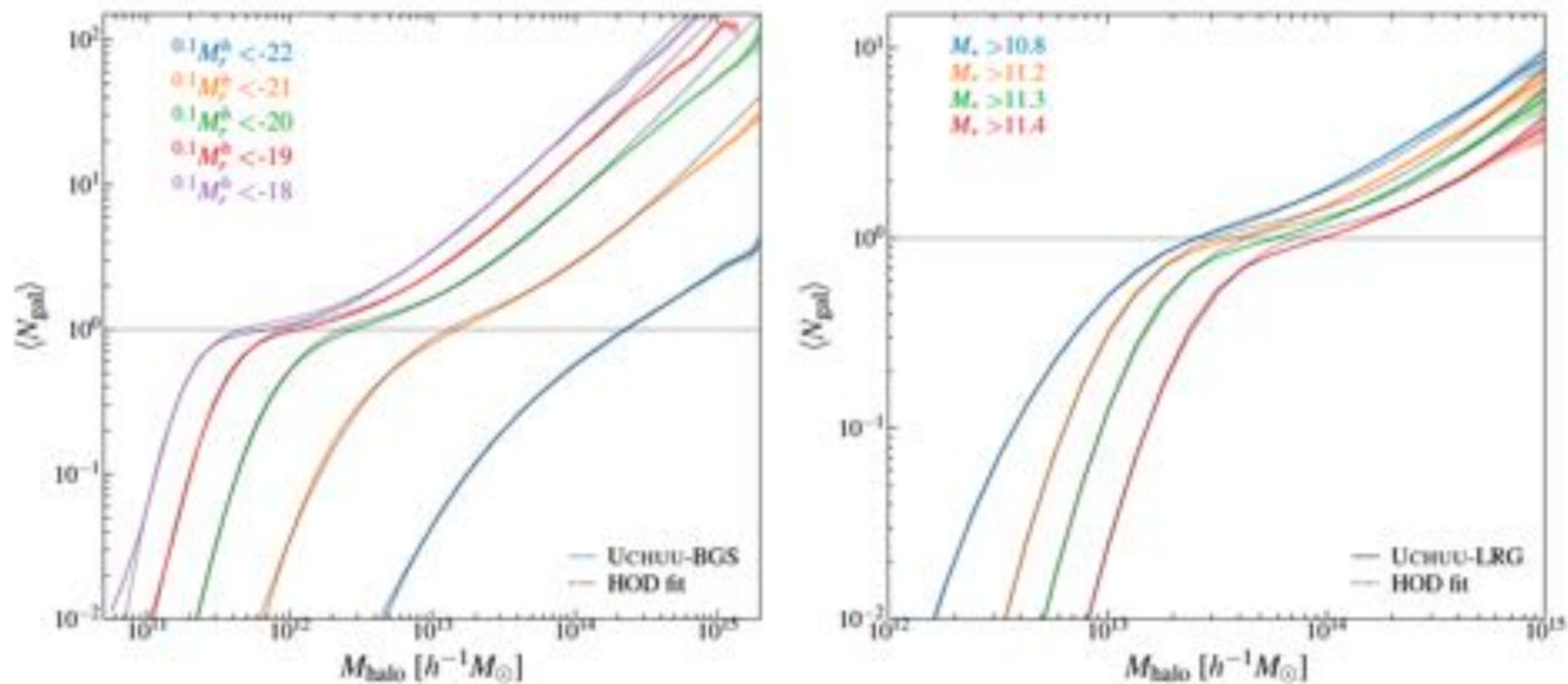
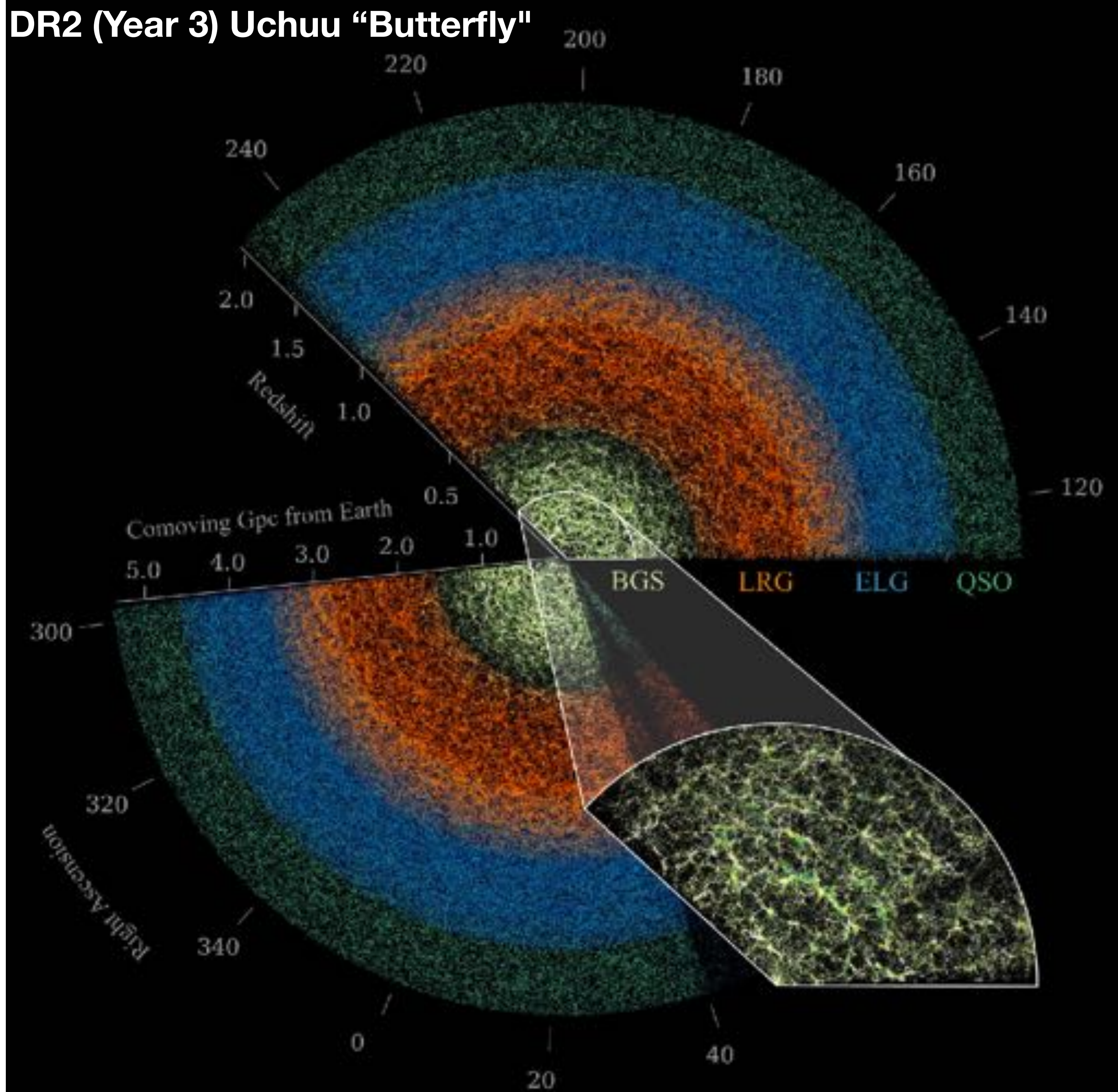


Fig. 14. Same as Figure 13 but showing the HODs for several BGS BRIGHT luminosity-threshold (left panel) and LRG stellar mass-threshold samples (right panel), selected from our UCHUU-DESI lightcones. The coloured curves show the HODs measured from the full-sky mock, where the sample is indicated in the legend, and the shaded area indicates the jackknife error, using 100 jackknife regions. The best-fitting 5-parameter HOD model for each sample is shown by the black dotted curves. HOD model parameters are provided in Tables 4 and 5 for the BGS and LRG samples, respectively.

DR2 (Year 3) Uchuu "Butterfly"



Keep an eye on arXiv for the upcoming **Year 3 Uchuu lightcone mock catalogs**, and clustering analysis:

- **Féernandez García et al.** — *BGS & LRG*
- **Rajeev, V. et al.** — *ELG & QSO*

They also include Uchuu DR1 mocks.



DESI DR2 Results: Measurements of Baryon Acoustic Oscillations and Cosmological Constraints

arXiv:2503.14738

Enrique Paillas (on behalf of the DESI Collaboration)
Steward Observatory
University of Arizona

APS Meeting
Anaheim, CA
Mar 2025

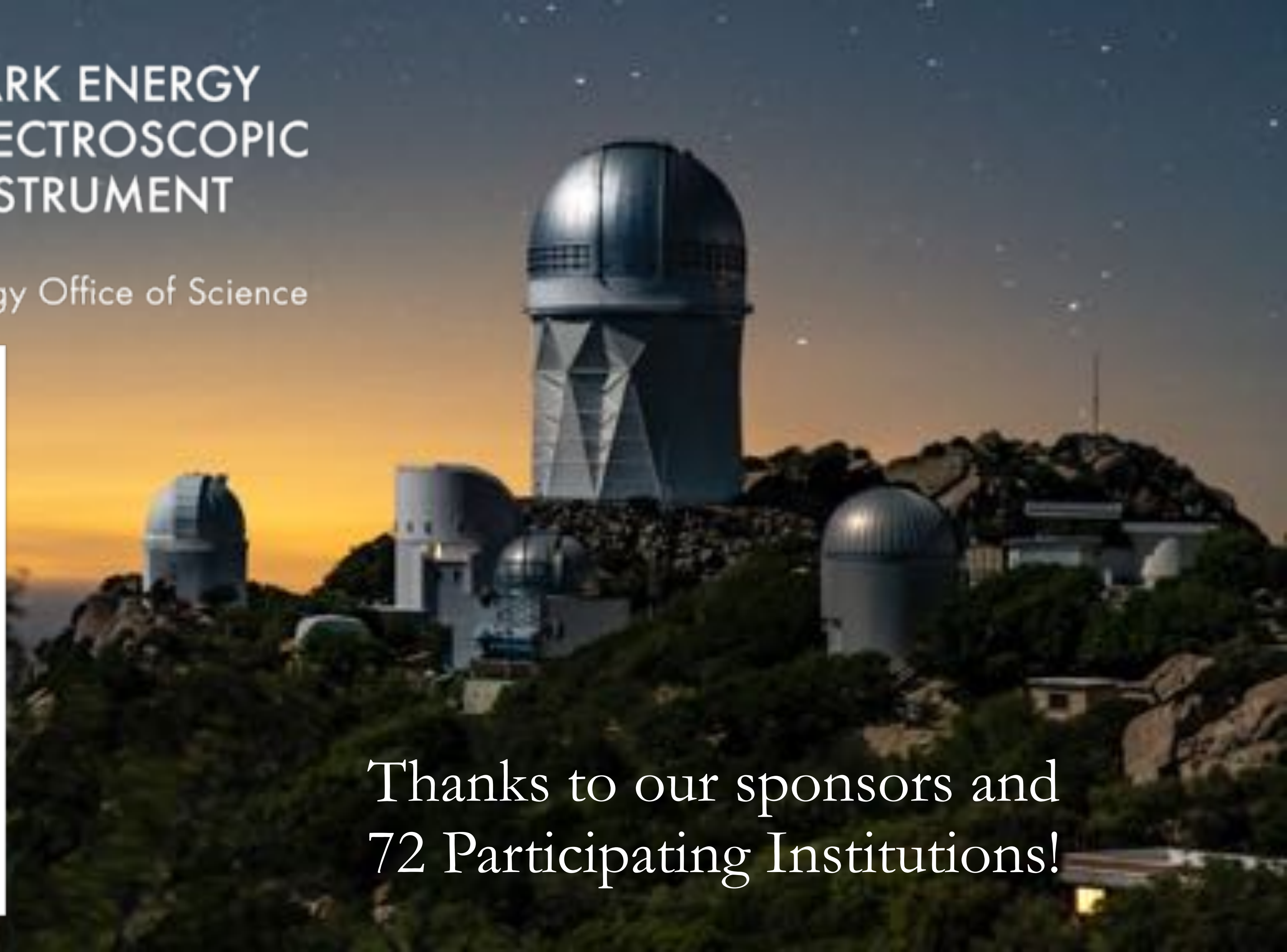


DARK ENERGY SPECTROSCOPIC INSTRUMENT

U.S. Department of Energy Office of Science



Thanks to our sponsors and
72 Participating Institutions!



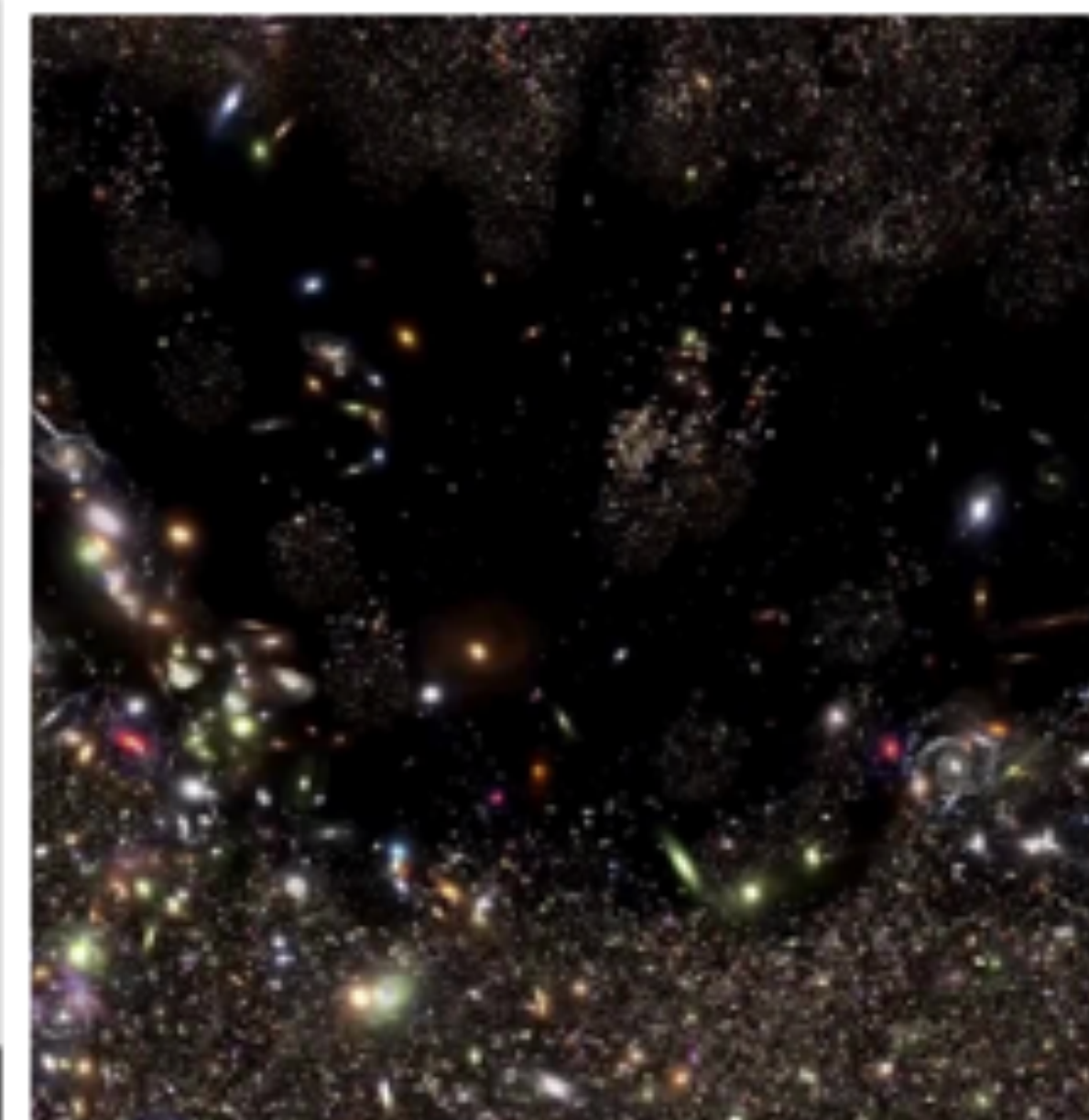
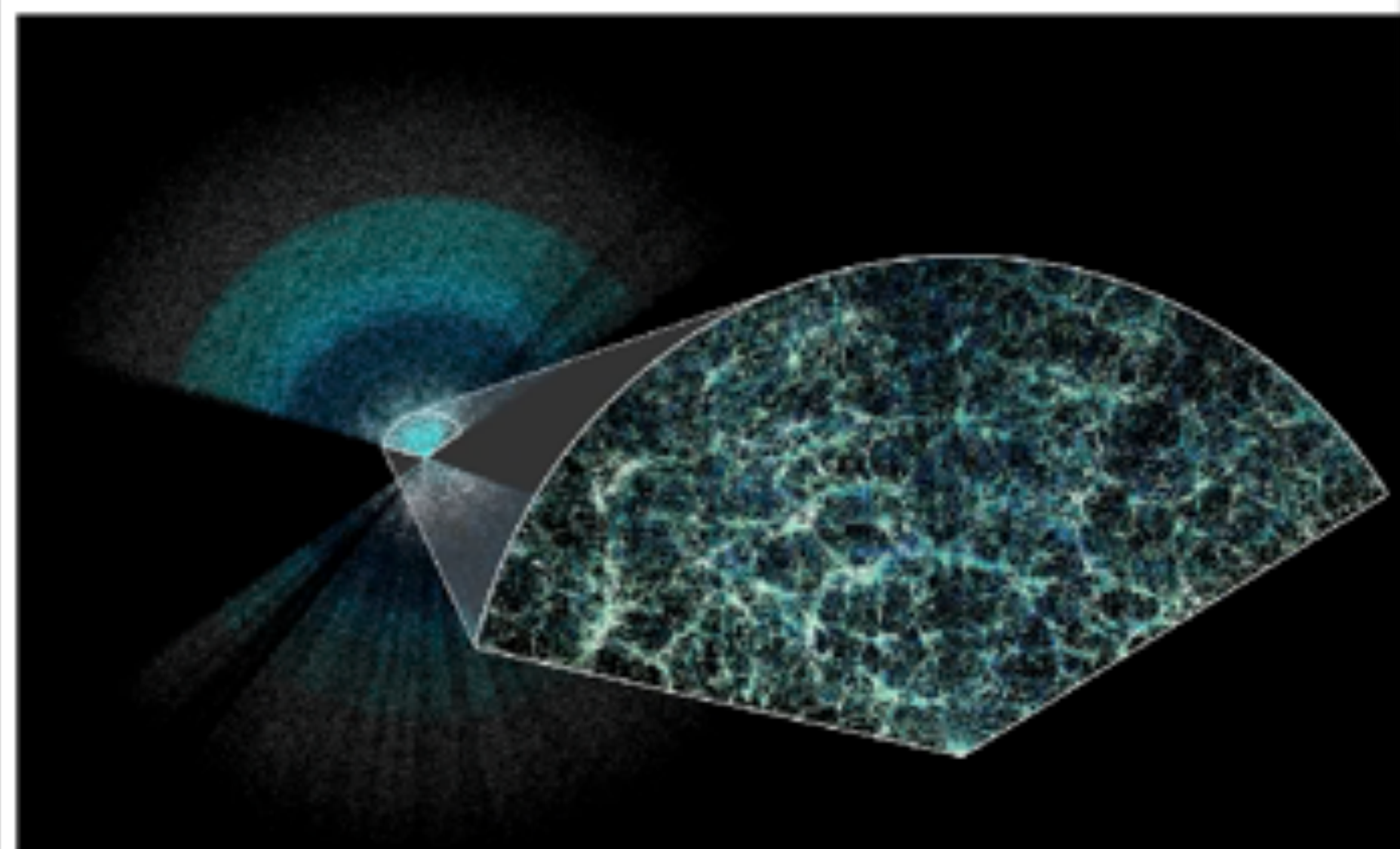


DARK ENERGY SPECTROSCOPIC INSTRUMENT

U.S. Department of Energy Office of Science

New 3D cosmic map raises questions over future of universe, scientists say

Researchers say findings from map with three times more galaxies than previous efforts could challenge standard idea of dark energy



The New York Times

A Tantalizing 'Hint' That Astronomers Got Dark Energy All Wrong

Scientists may have discovered a major flaw in their understanding of that mysterious cosmic force. That could be good news for the fate of the universe.

2024 Biggest Breakthroughs in Physics

16:45





DARK ENERGY
SPECTROSCOPIC
INSTRUMENT

U.S. Department of Energy Office of Science

The DESI DR2 sample

Redshifts for the BAO analysis

| Tracer | DR1 | DR2 |
|--------|-----------|-------------------|
| BGS | 300.043 | 1.188.526 |
| LRG | 2.138.627 | 4.468.483 |
| ELG | 2.432.072 | 6.534.844 |
| QSO | 1.223.391 | 2.062.839 |
| Total | 6.094.133 | 14.254.692 |

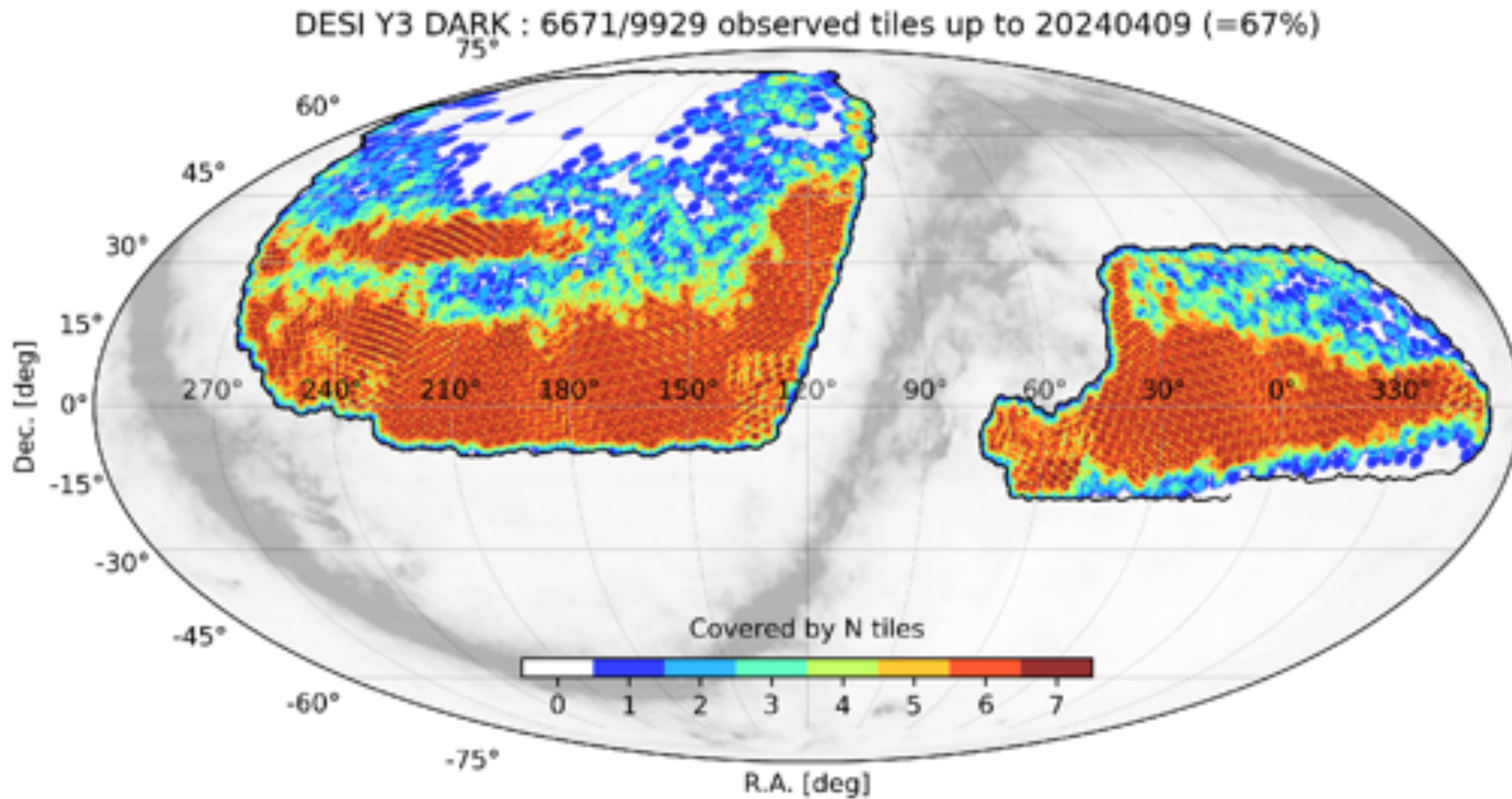
- Over 30M galaxy and quasar redshifts in *3 years of operation*, ~14M of which are used in this analysis.
- Compared to DR1 (~6M redshifts), DR2 represents a factor of *~2.4 improvement* in data volume.



DARK ENERGY
SPECTROSCOPIC
INSTRUMENT

The DESI DR2 sample

U.S. Department of Energy Office of Science



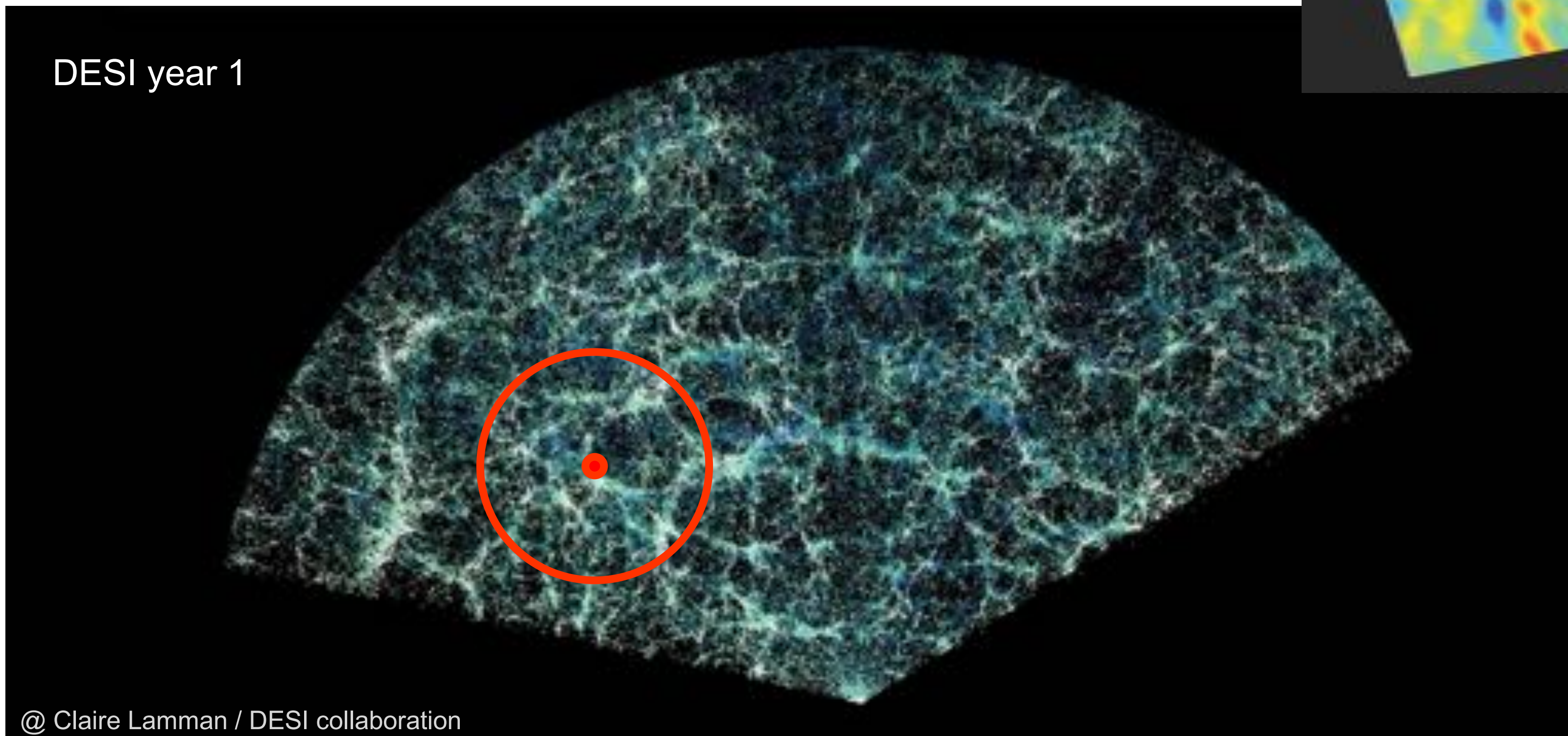
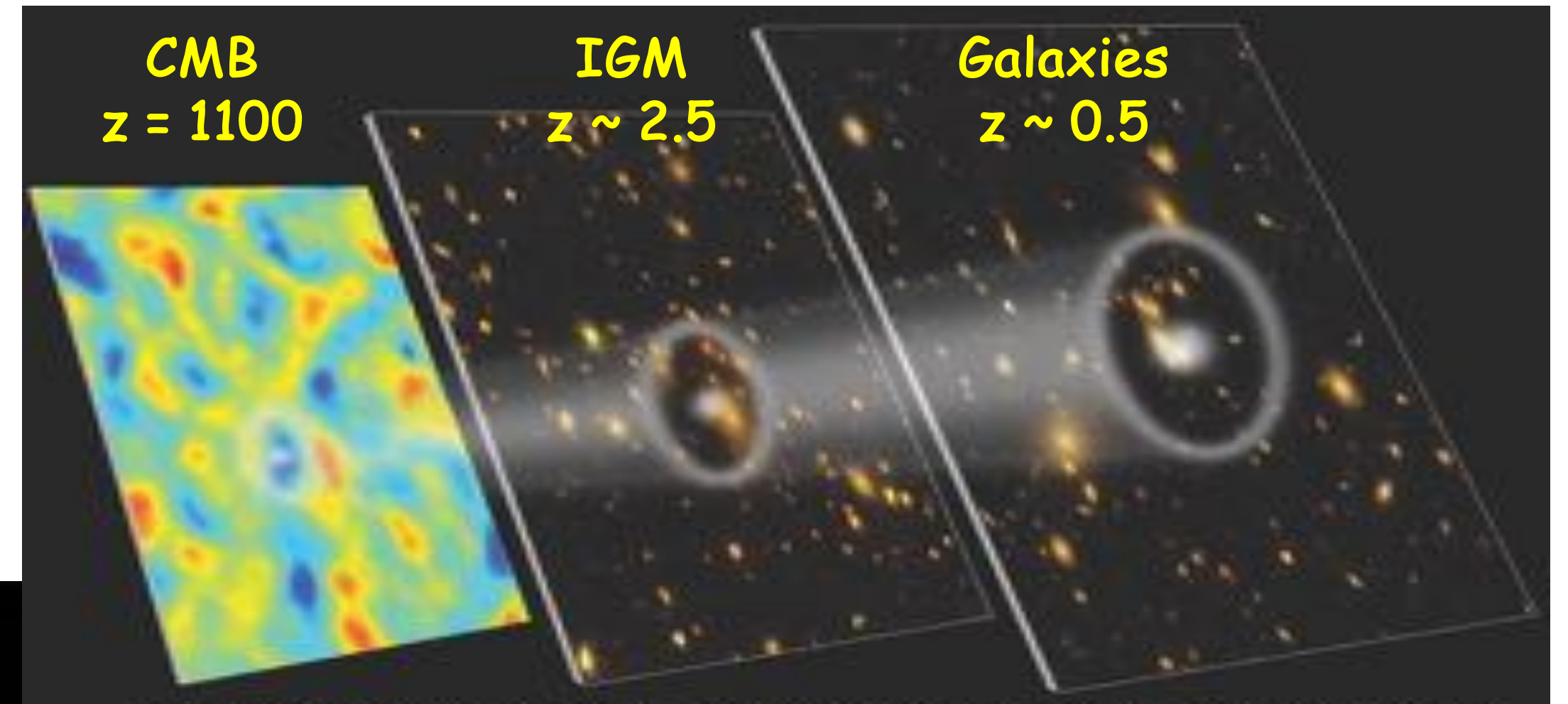


DARK ENERGY
SPECTROSCOPIC
INSTRUMENT

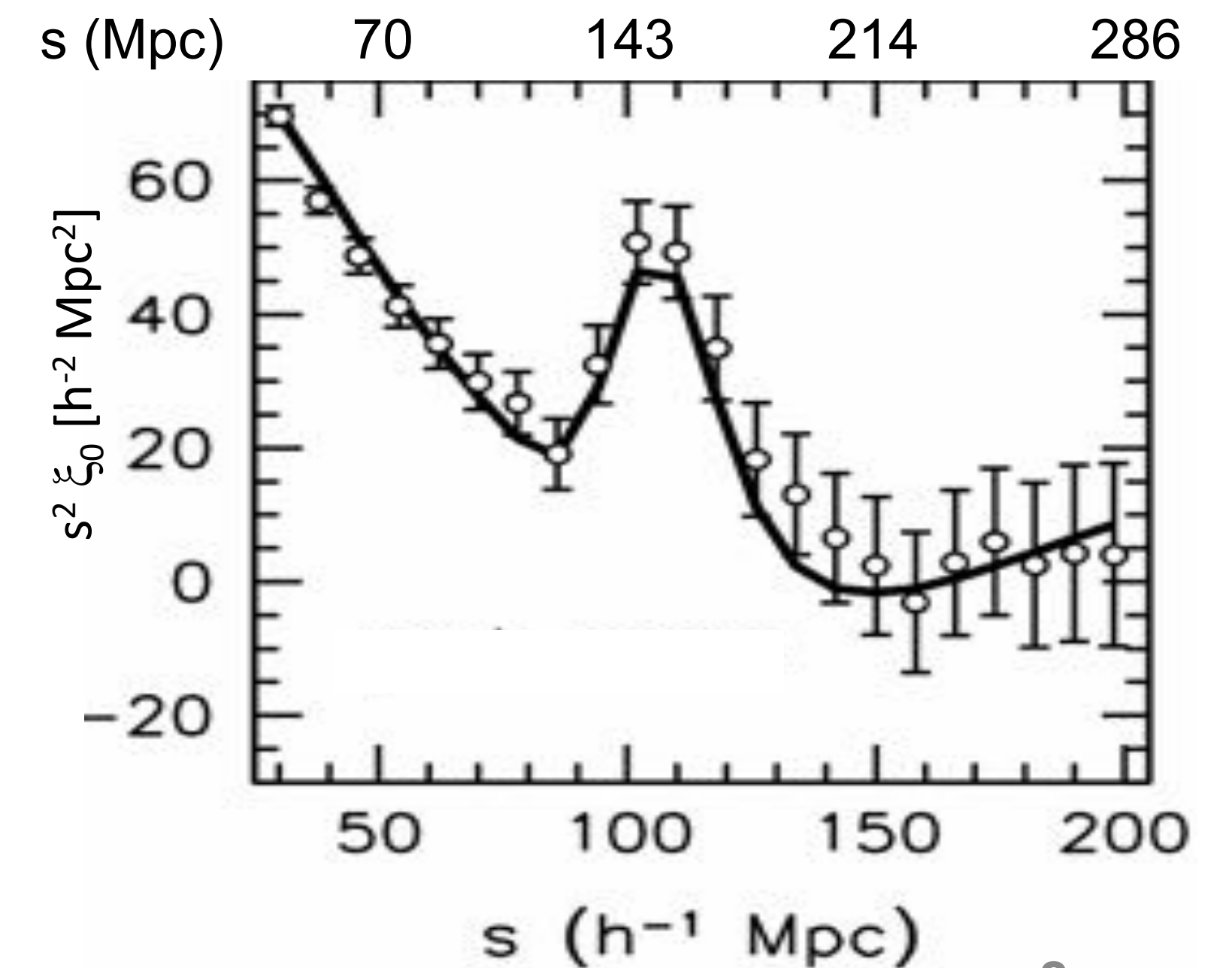
U.S. Department of Energy Office of Science

Baryon Acoustic Oscillations (BAO)

Imprint of fluctuations in primordial plasma
 → Standard Ruler to measure distances



@ Claire Lamman / DESI collaboration



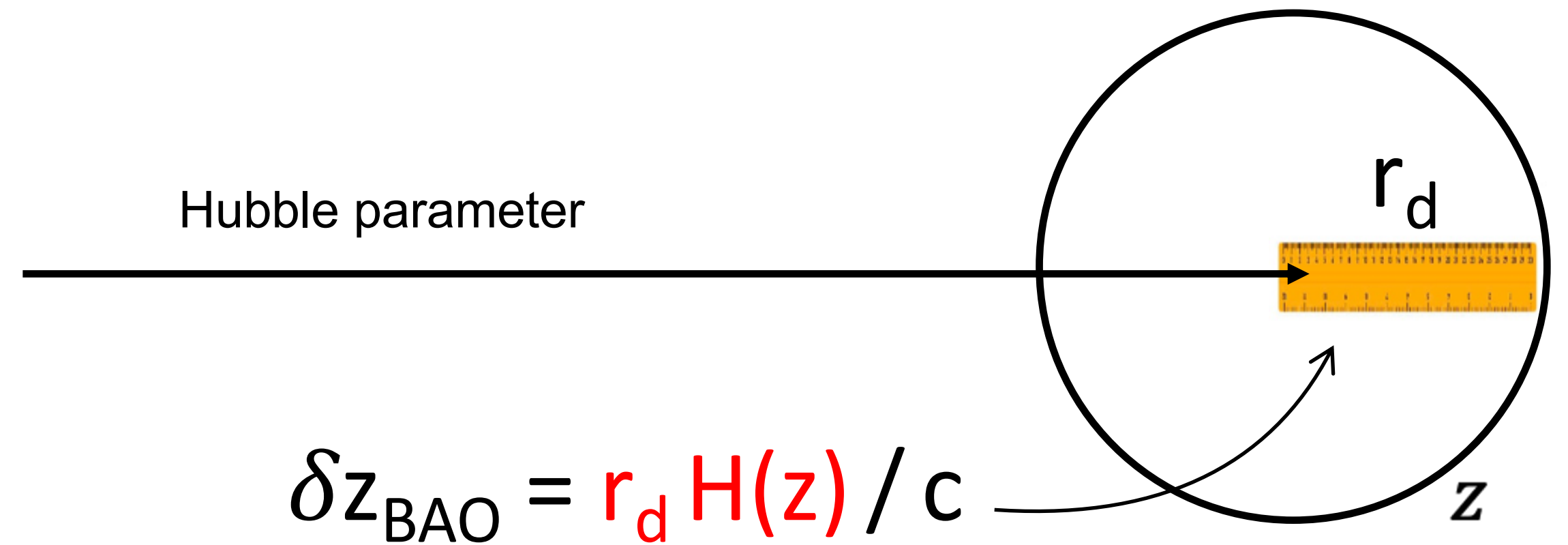
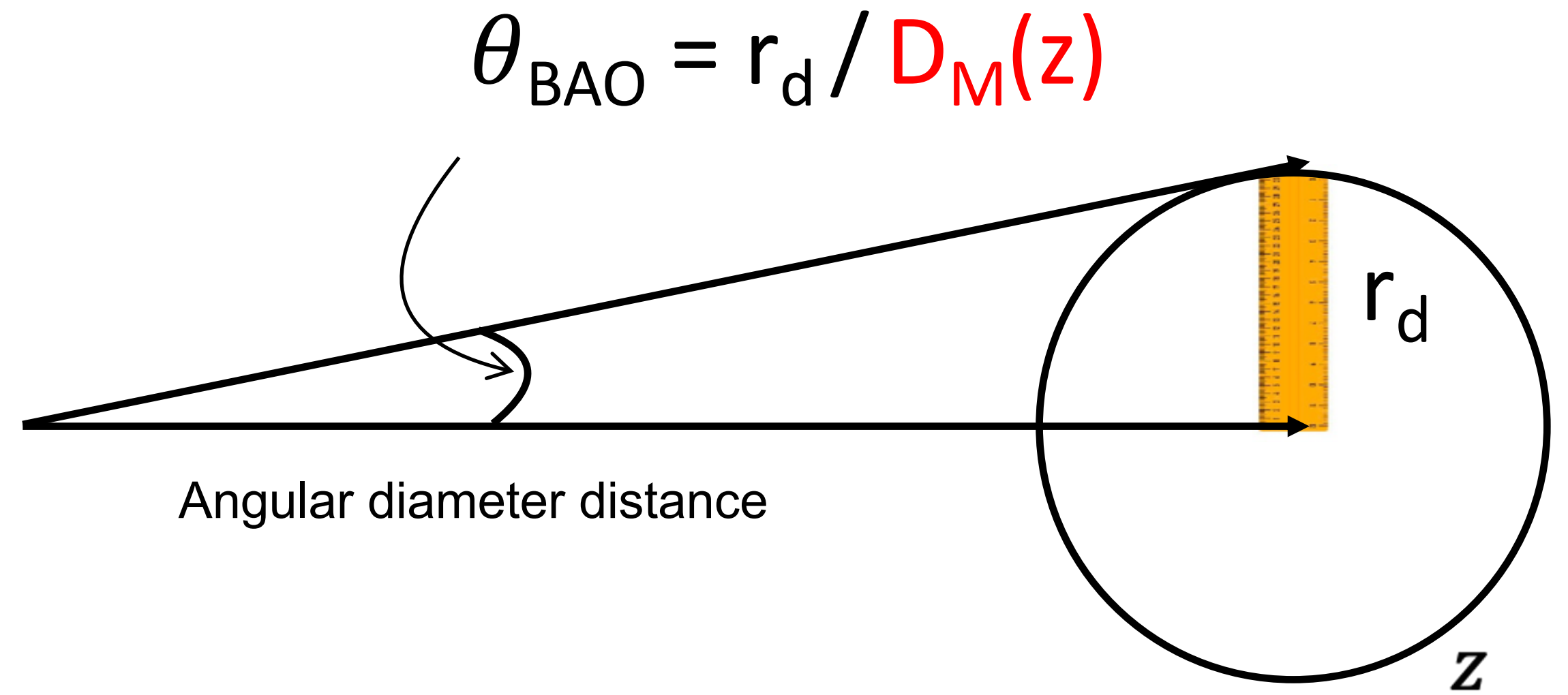
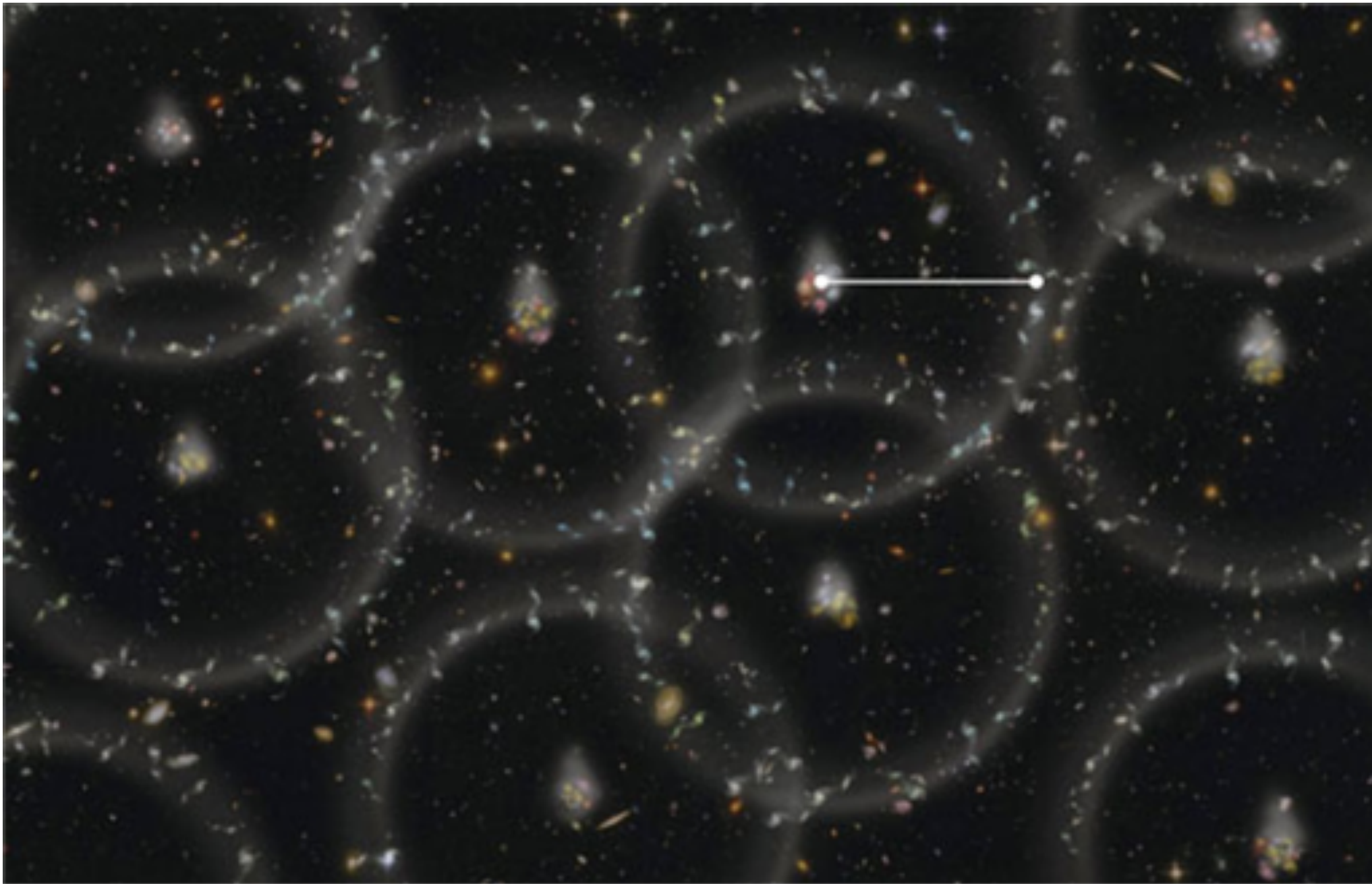
The BAO standard ruler



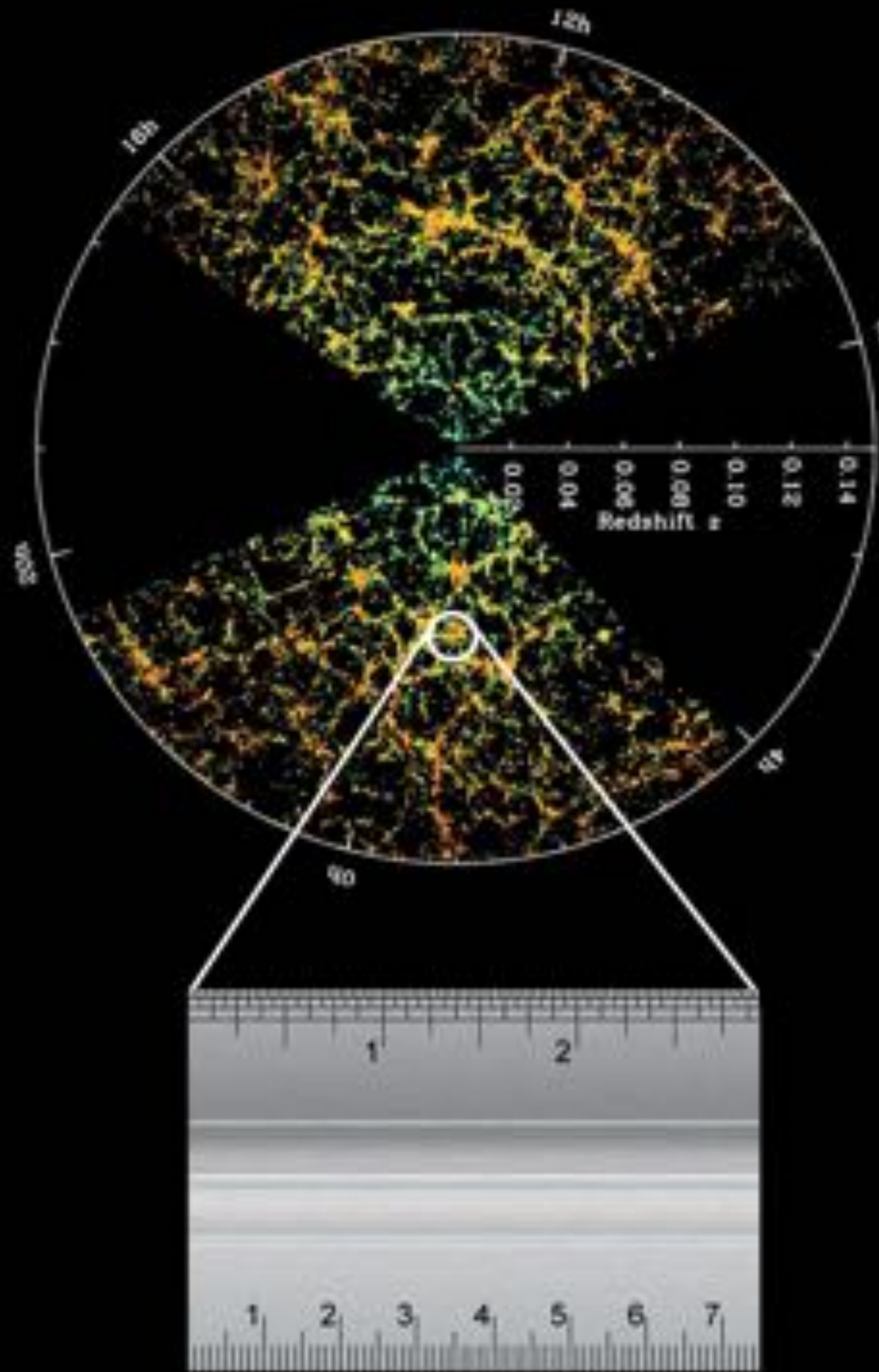
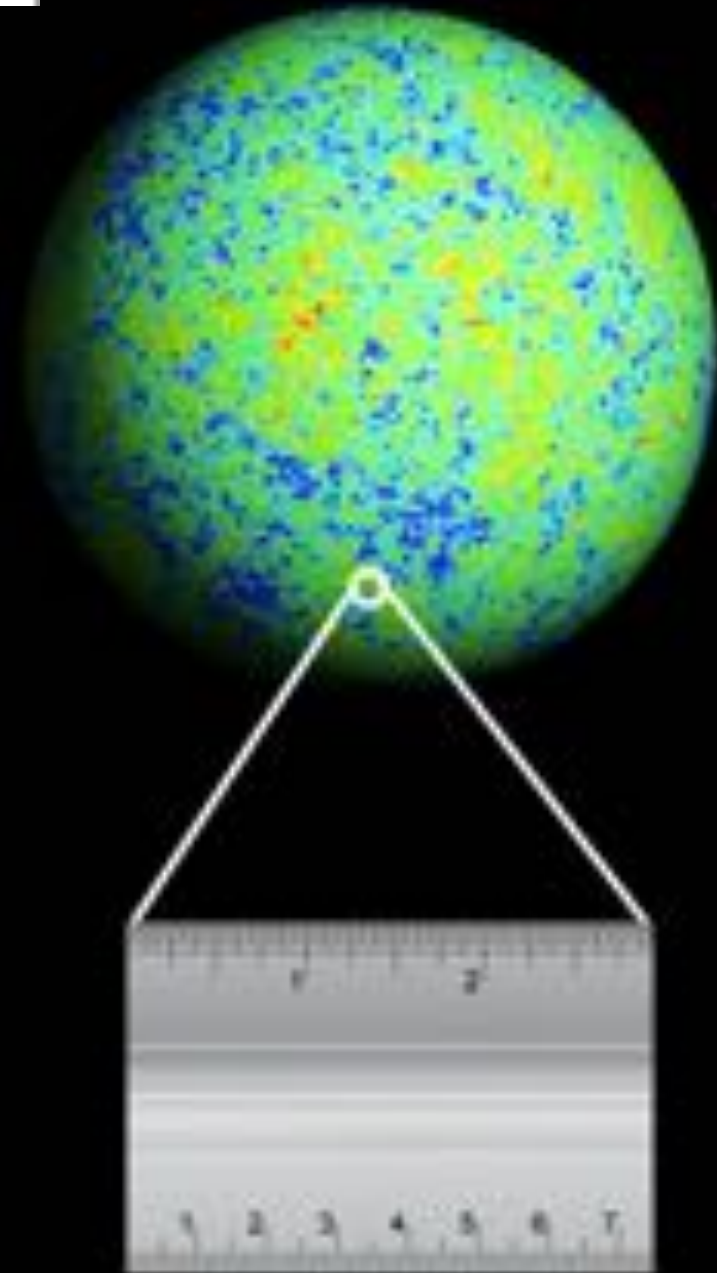
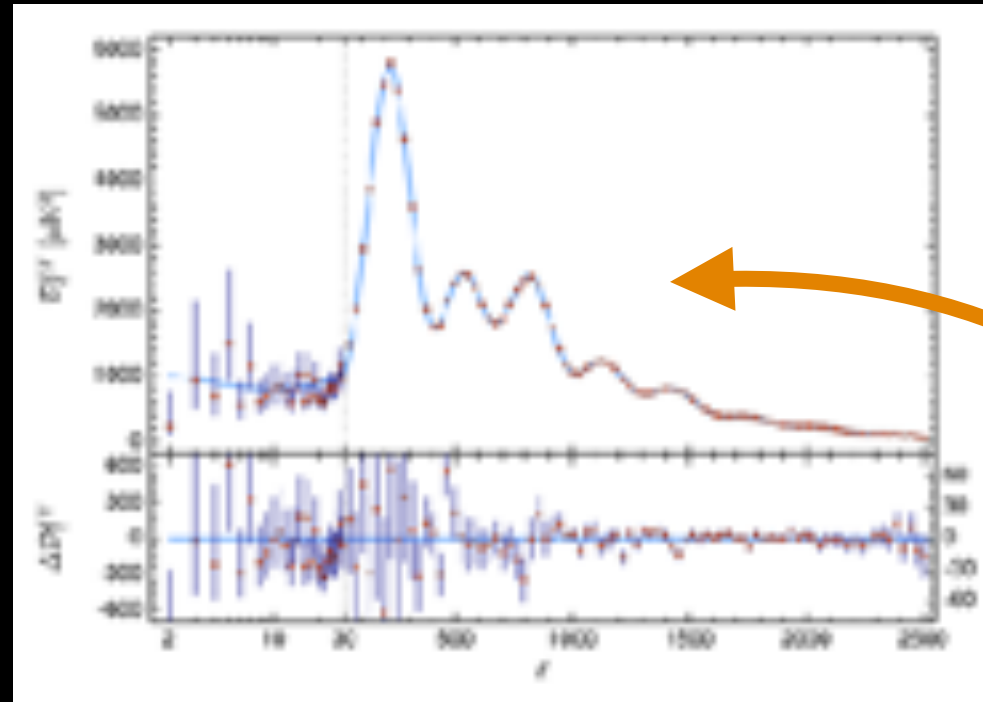
DARK ENERGY
SPECTROSCOPIC
INSTRUMENT

U.S. Department of Energy Office of Science

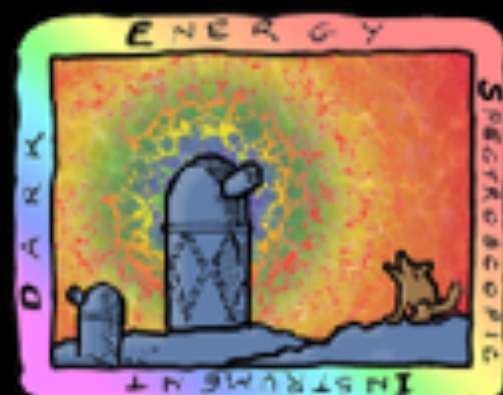
Artist's view of BAO



$D_M(z)$ and $H(z)$ encode **expansion history** of the Universe



An external calibration on r_d allows us to constrain H_0 with BAO data.



DARK ENERGY SPECTROSCOPIC INSTRUMENT

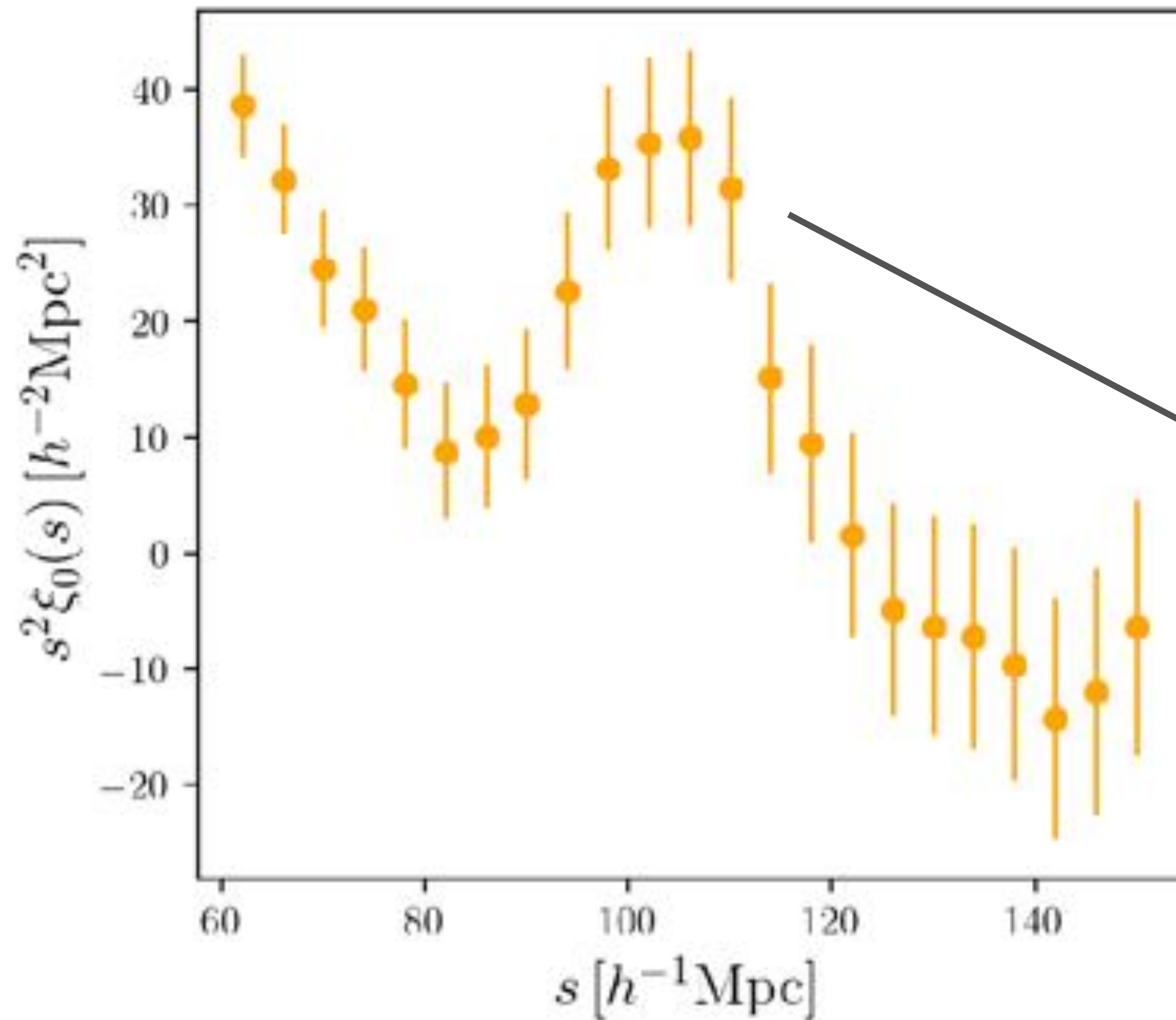


DARK ENERGY
SPECTROSCOPIC
INSTRUMENT

U.S. Department of Energy Office of Science

Clustering from galaxies and quasars

Clustering amplitude



Galaxy pair separation

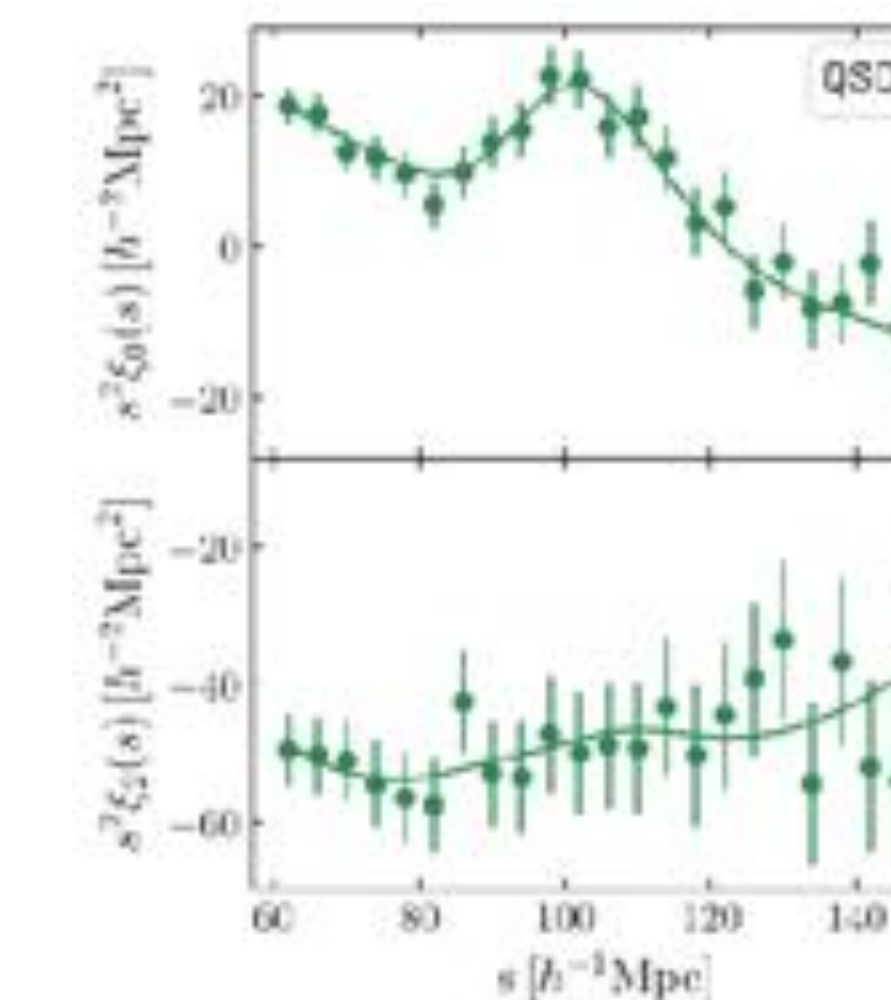
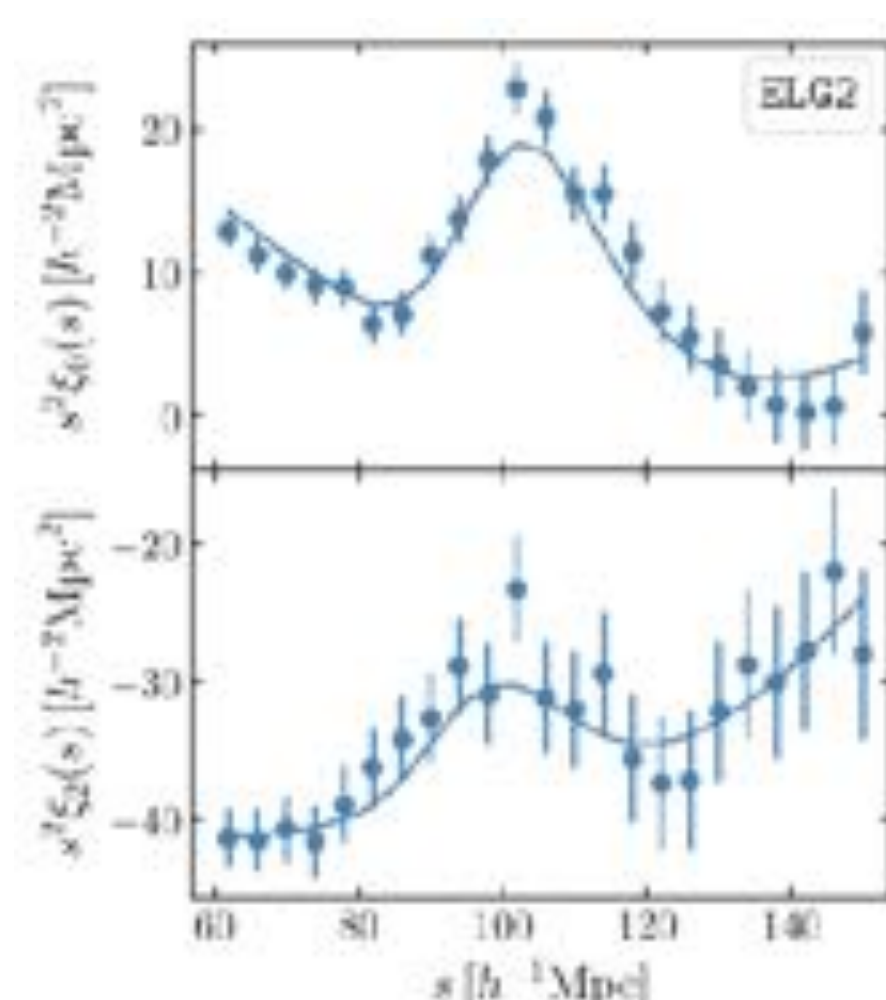
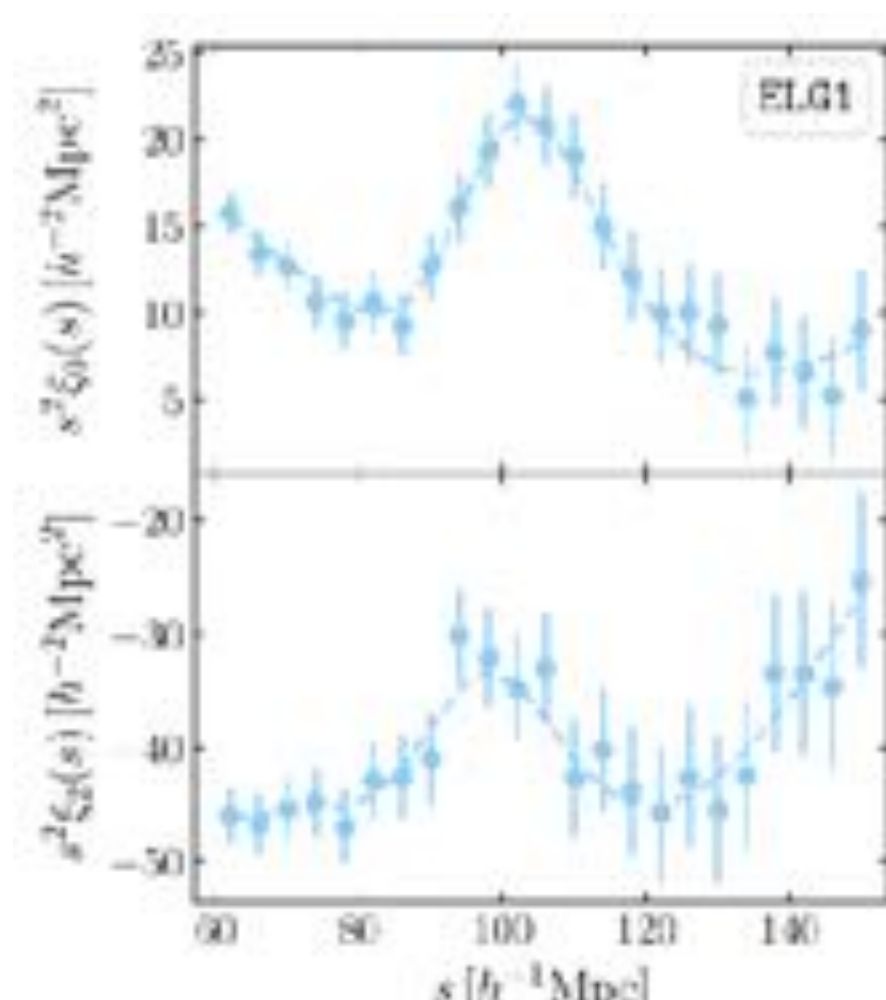
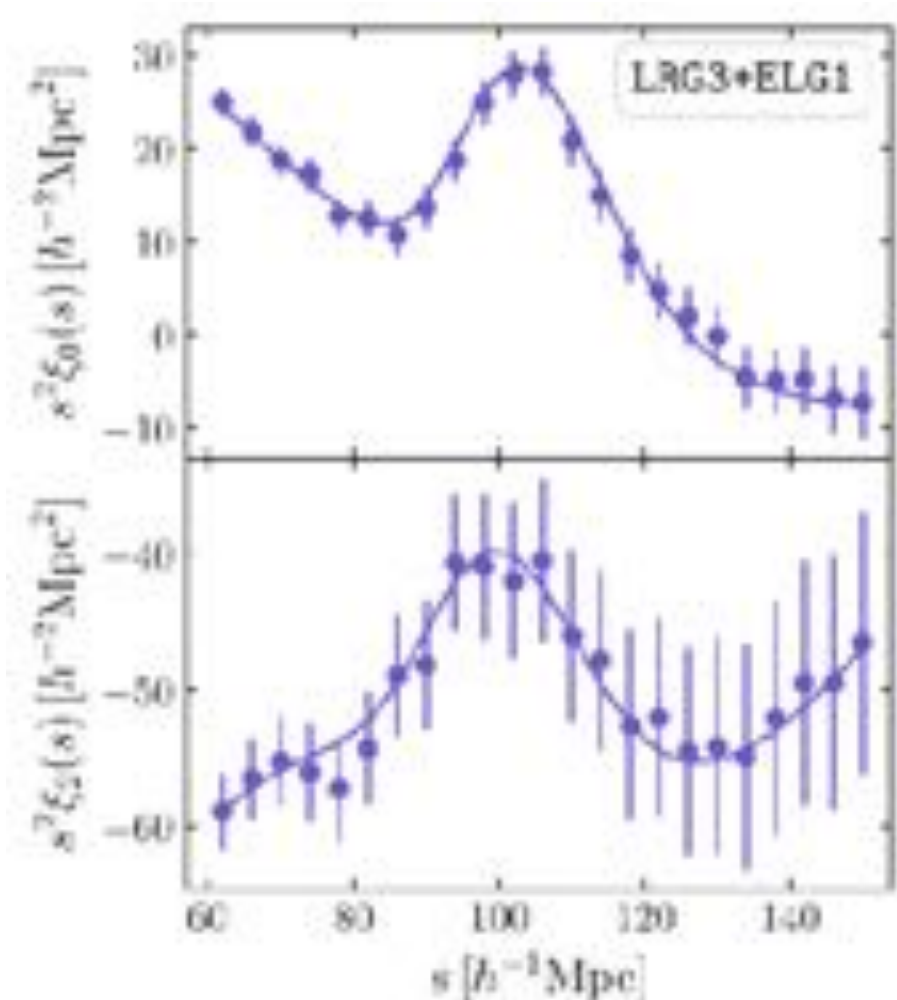
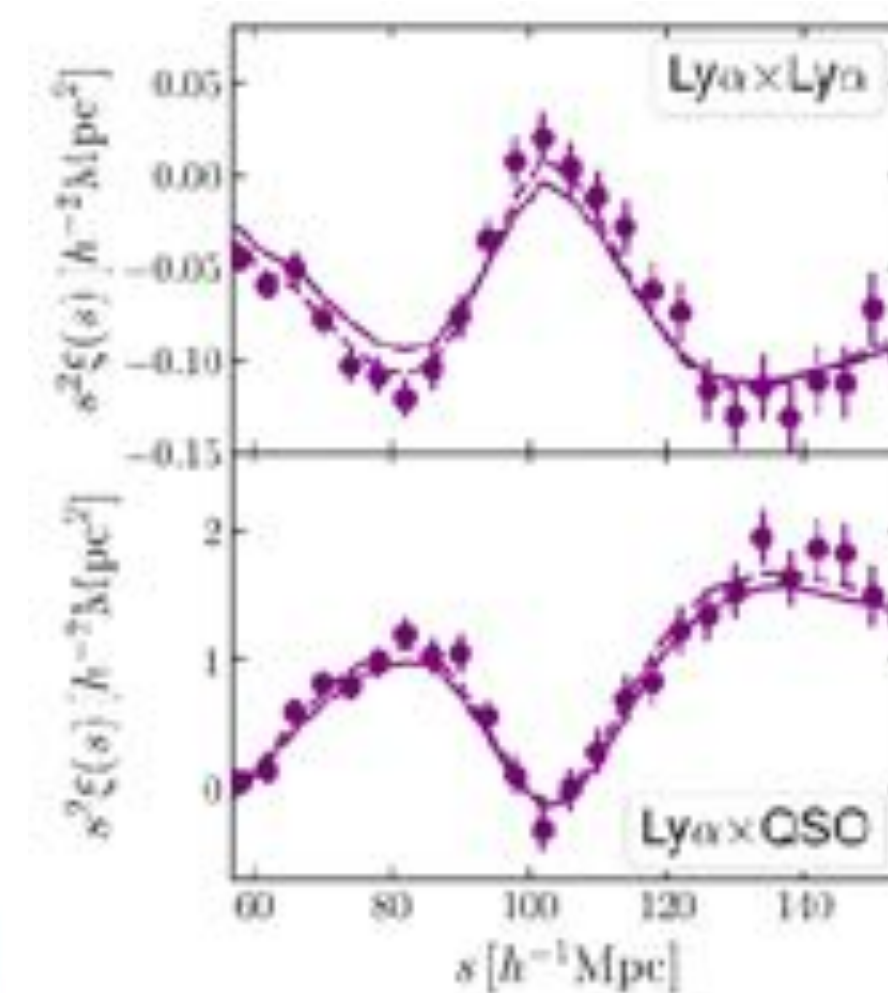
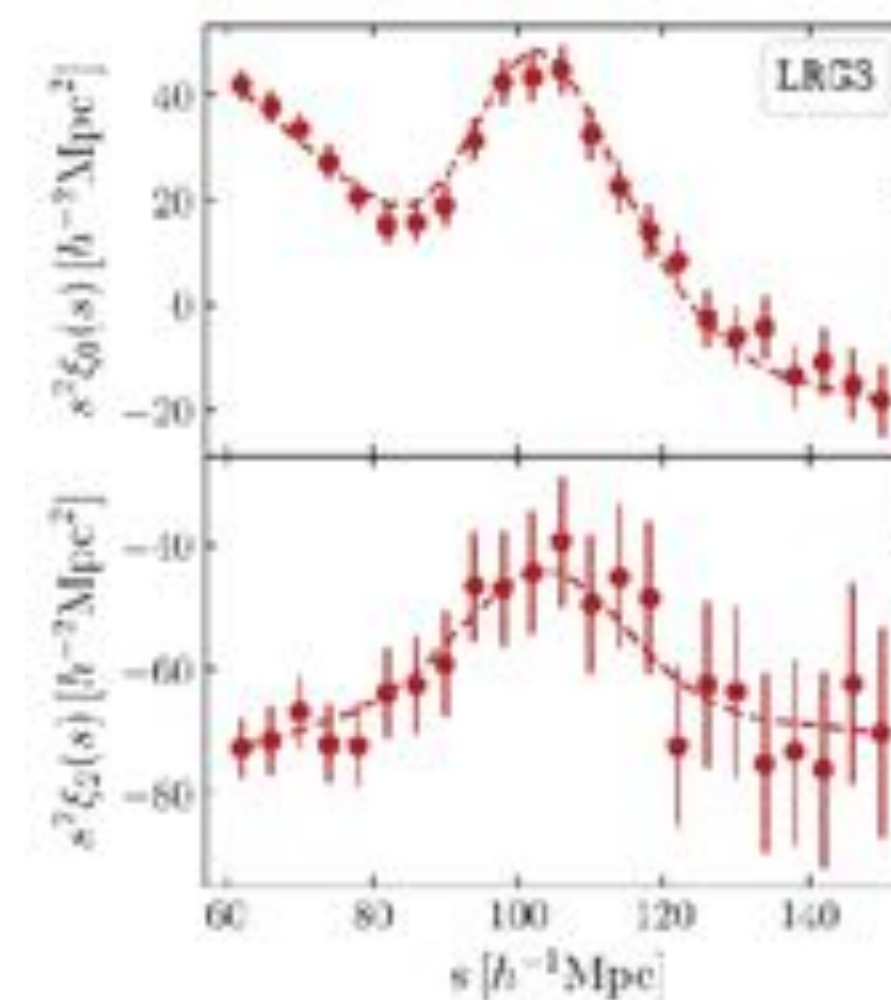
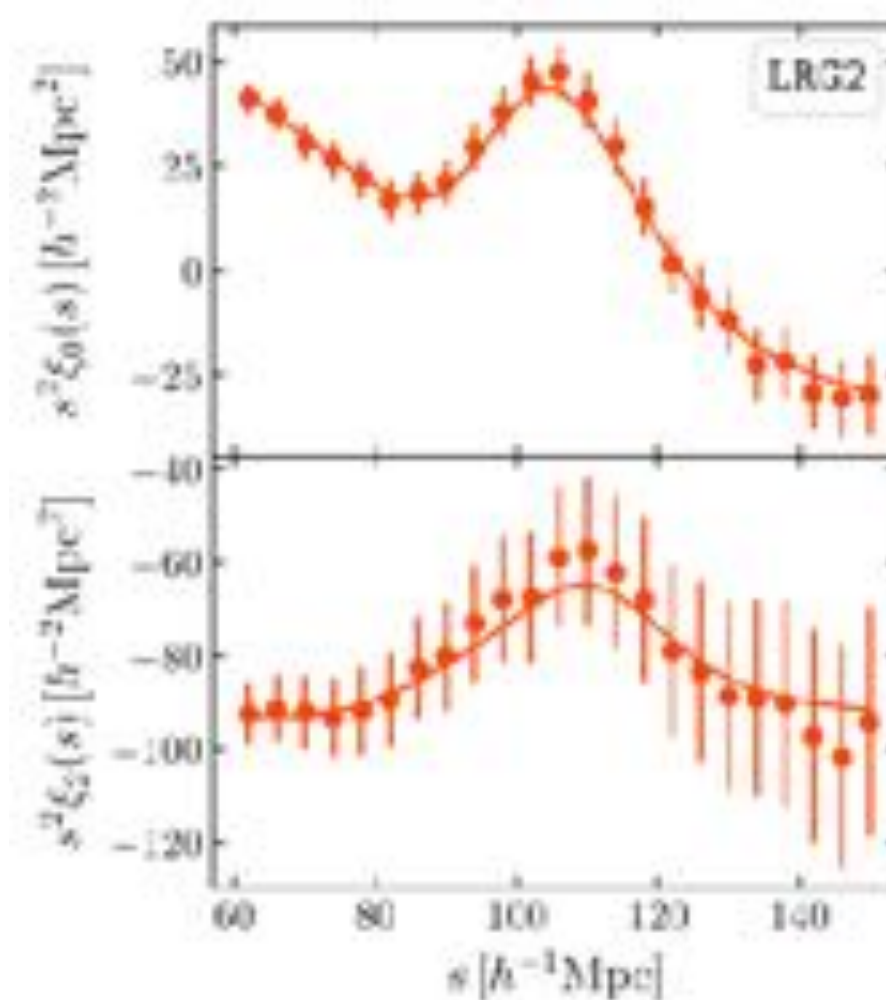
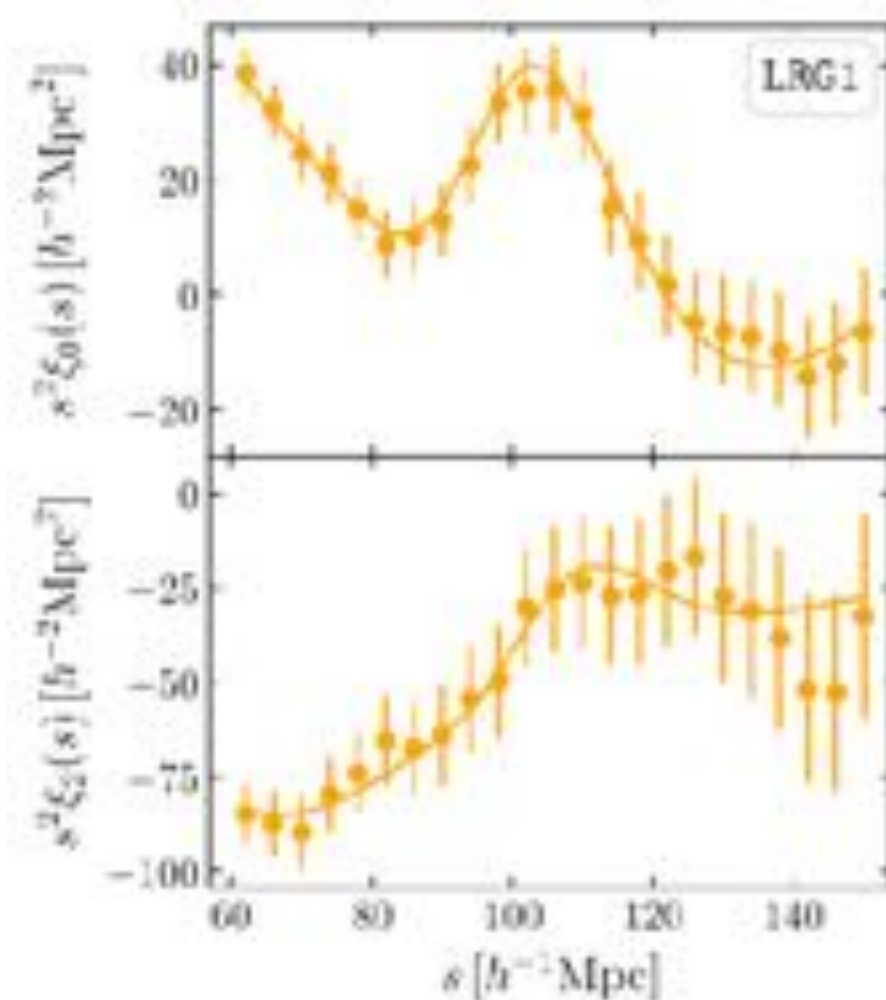
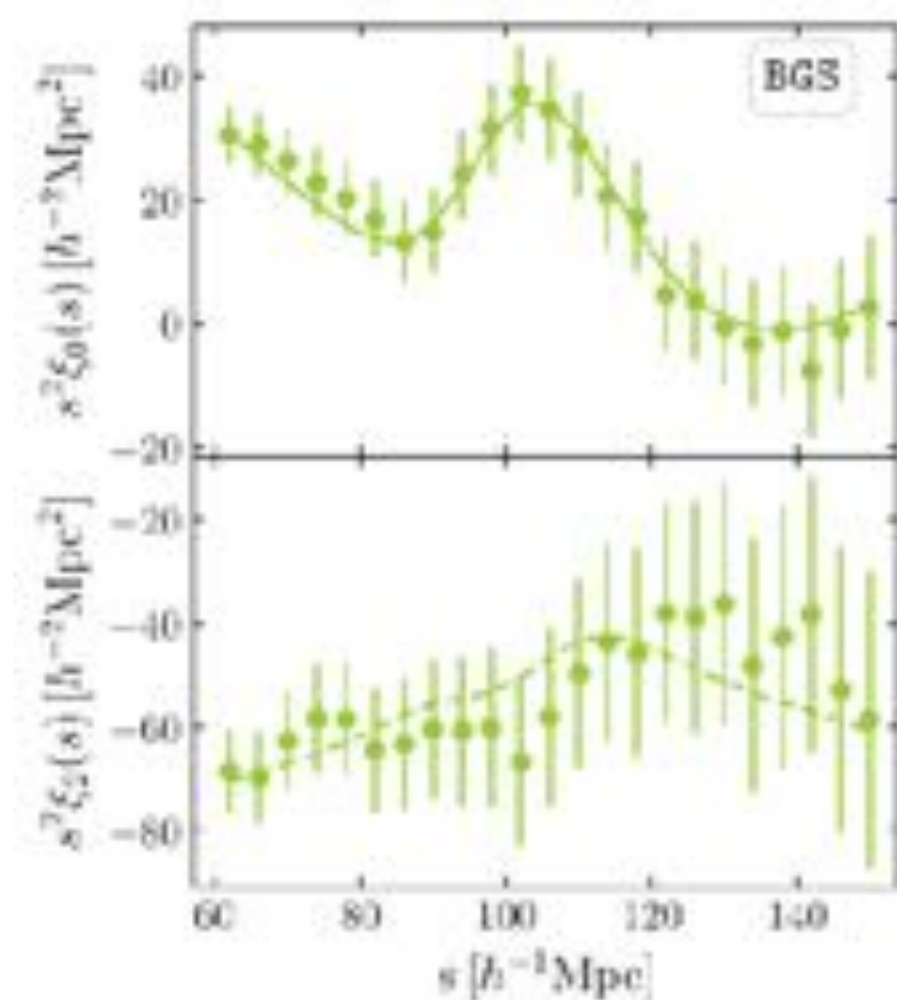
- The **correlation function** measures clustering as a function of scale: $\xi(r) = \langle \delta(x) \delta(x+r) \rangle$
- The BAO appears as a distinct peak around $100 h^{-1} \text{Mpc}$ (or wiggles in the *power spectrum*).



DARK ENERGY
SPECTROSCOPIC
INSTRUMENT

DESI DR2 Clustering Measurements

U.S. Department of Energy Office of Science



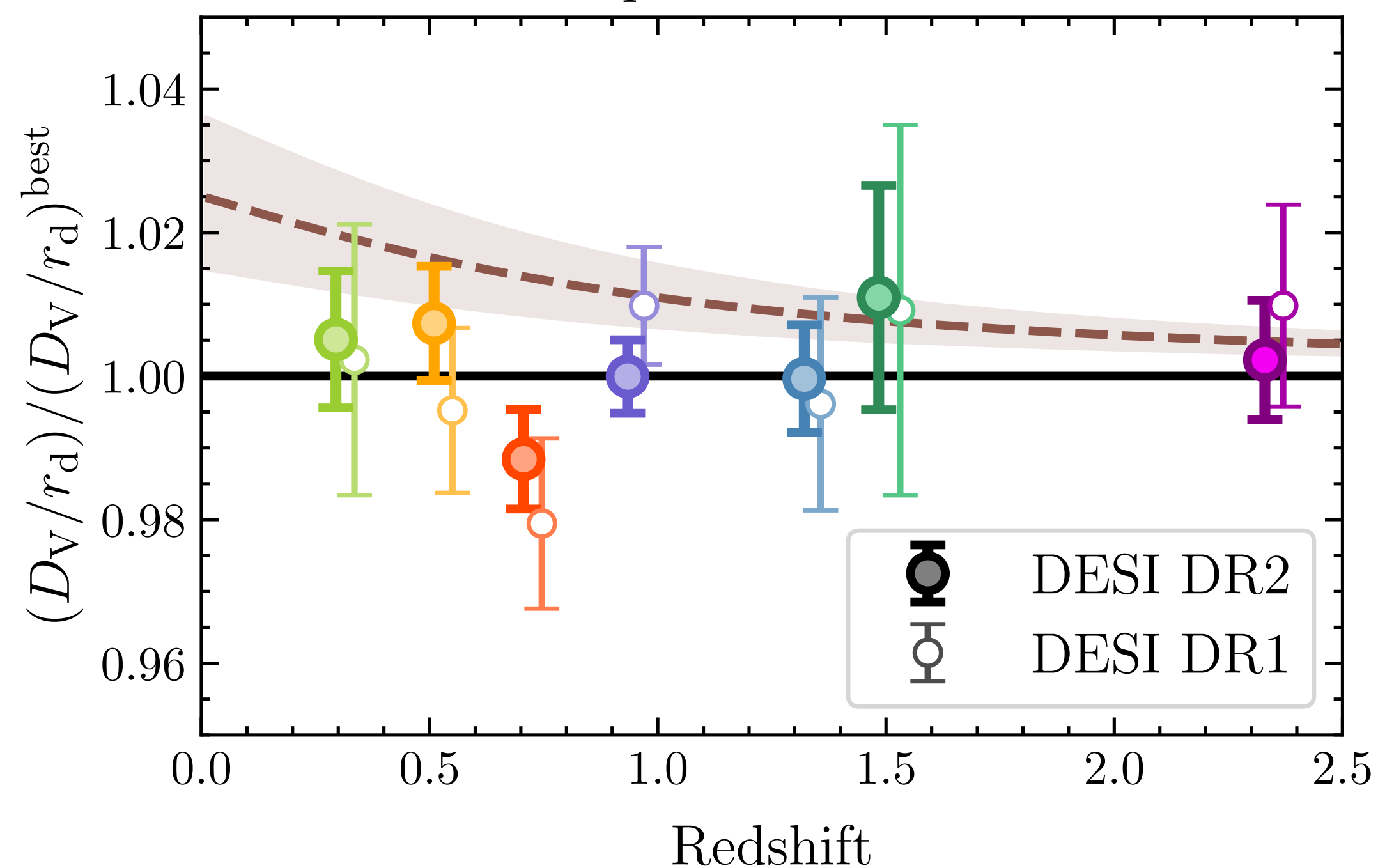


DARK ENERGY
SPECTROSCOPIC
INSTRUMENT

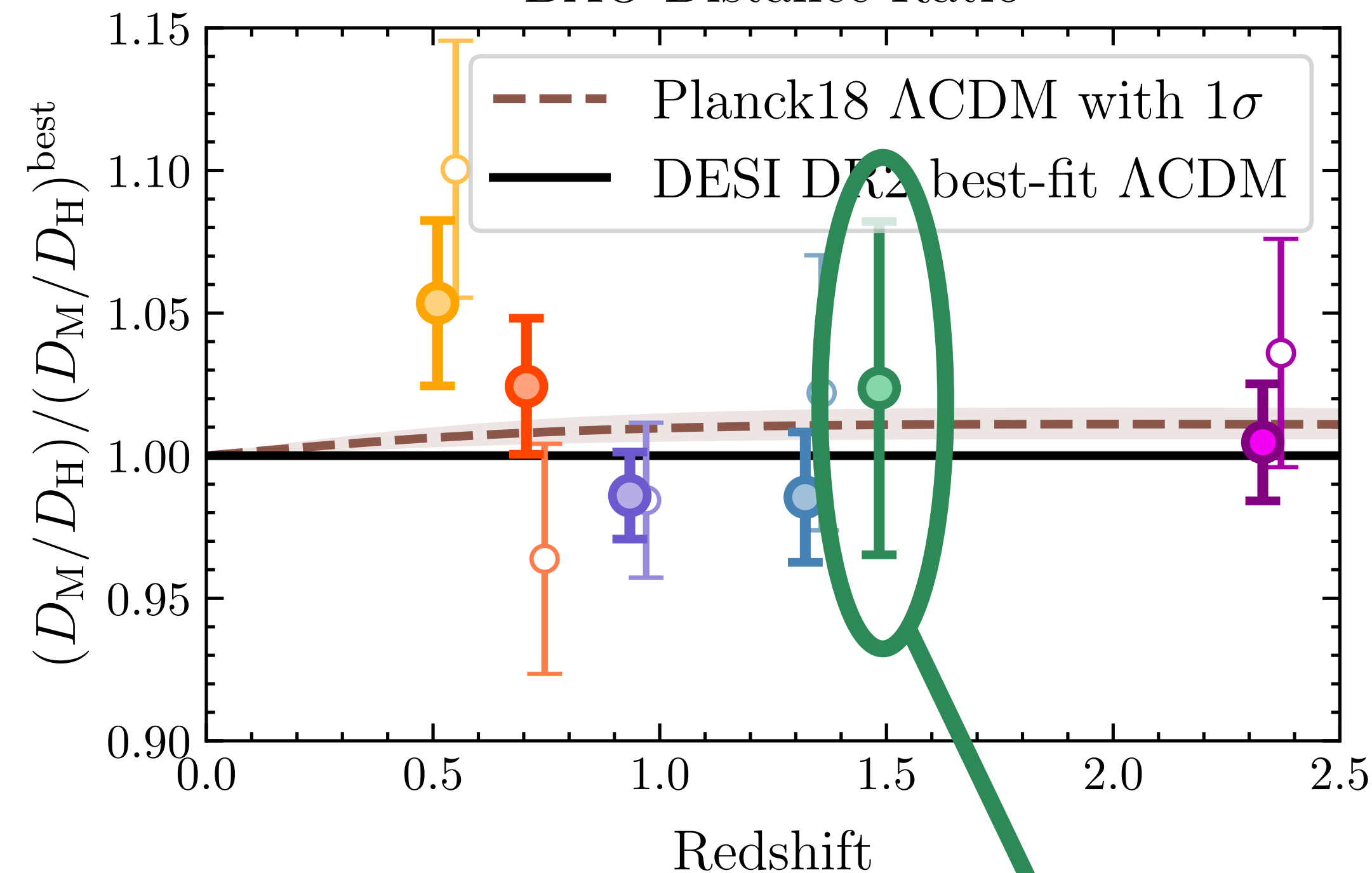
BAO Distance Measurements

U.S. Department of Energy Office of Science

Isotropic BAO Distance



BAO Distance Ratio



New QSO distance
ratio measurement

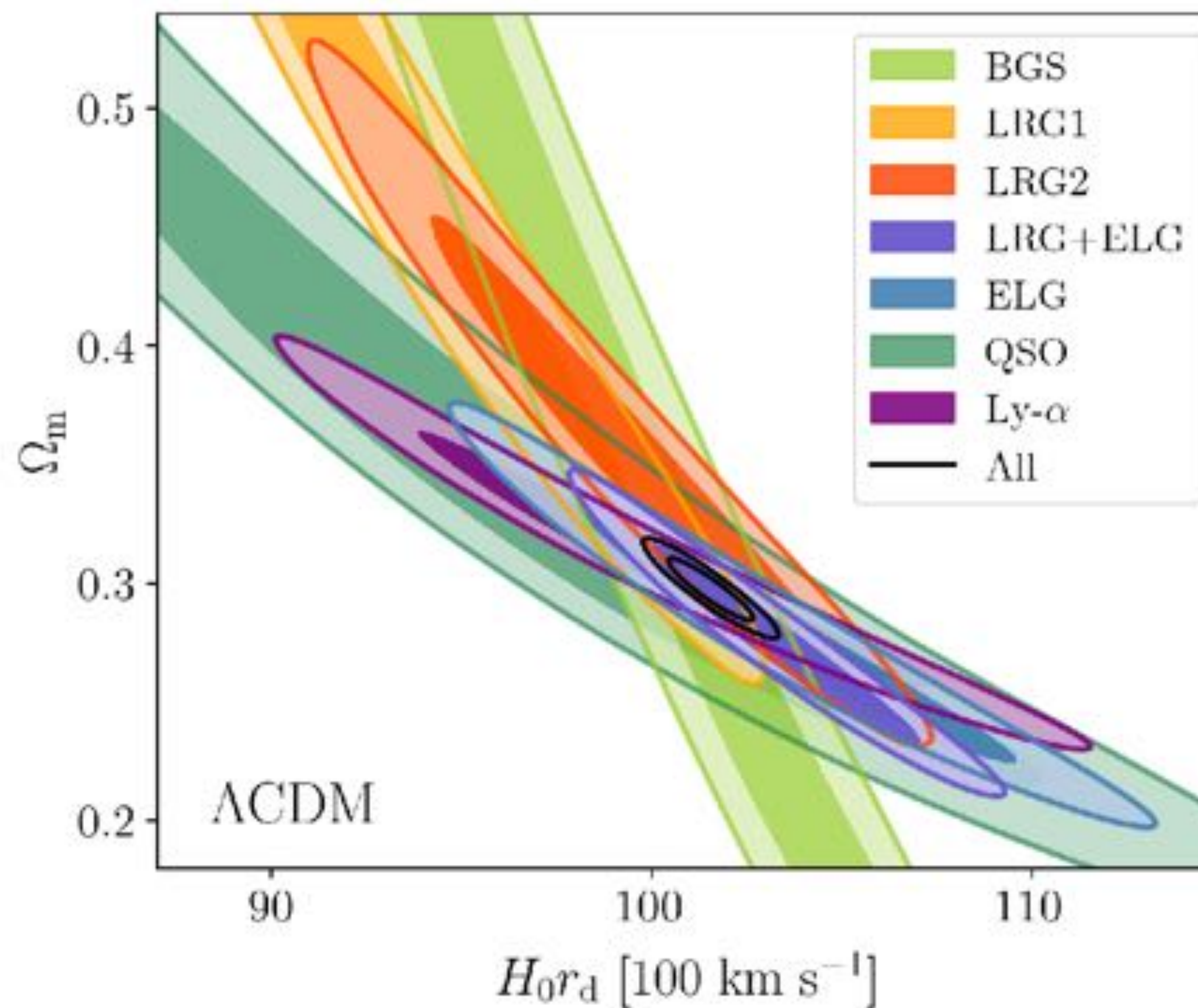


DARK ENERGY
SPECTROSCOPIC
INSTRUMENT

U.S. Department of Energy Office of Science

Mutual Consistency of DESI Tracers

- From low to high redshift, the increase on the effective redshift of the sample induces a counter clockwise shift in the degeneracy direction.
- The results from each individual tracer are mutually consistent and complementary in providing tighter constraints.

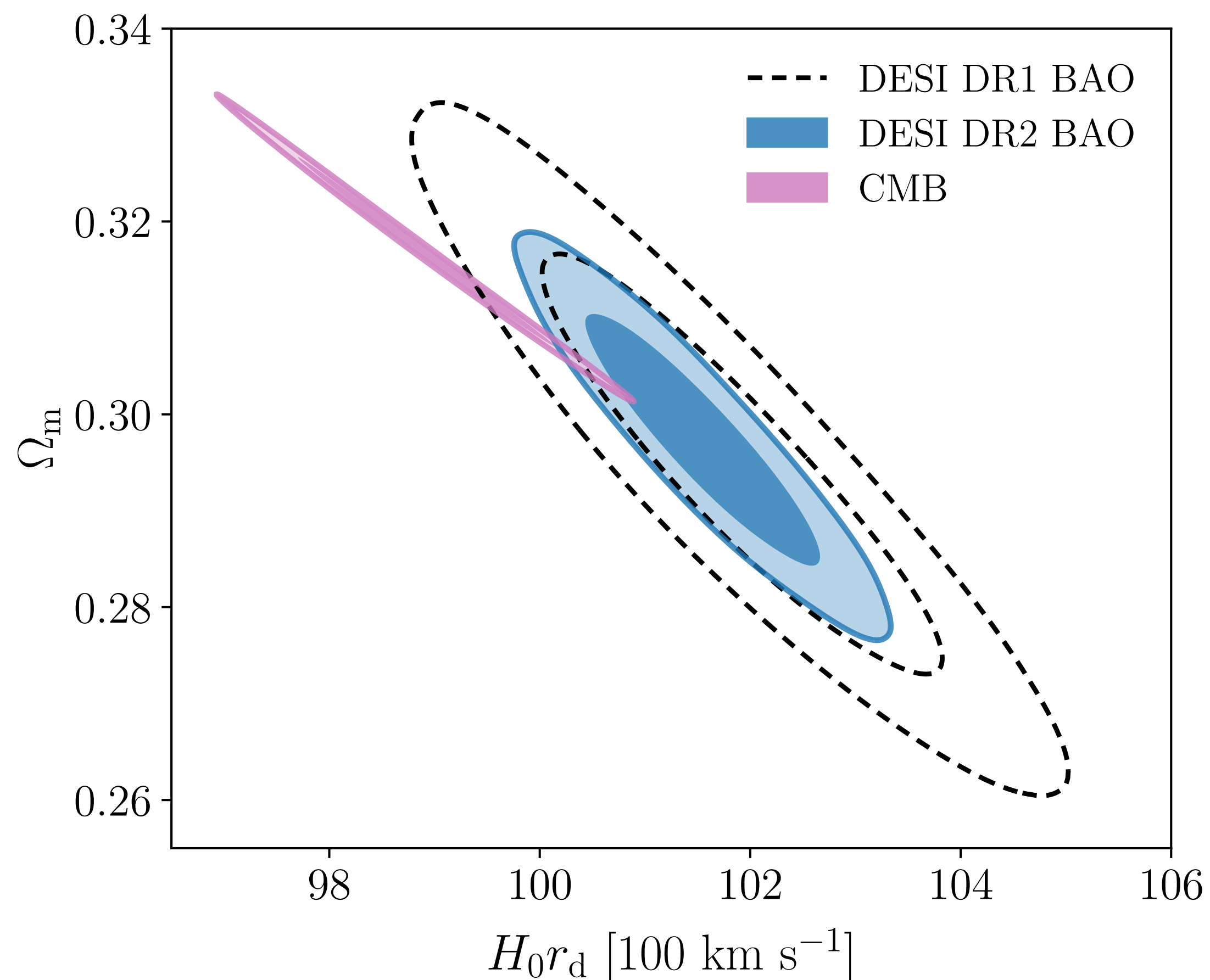




DARK ENERGY
SPECTROSCOPIC
INSTRUMENT

U.S. Department of Energy Office of Science

Constraints under Λ CDM



- 40% Improvement in the precision on Ω_m and hr_d compared to DR1.
- Discrepancy between BAO and CMB has increased: 1.9σ (DR1) \rightarrow 2.3σ (DR2).

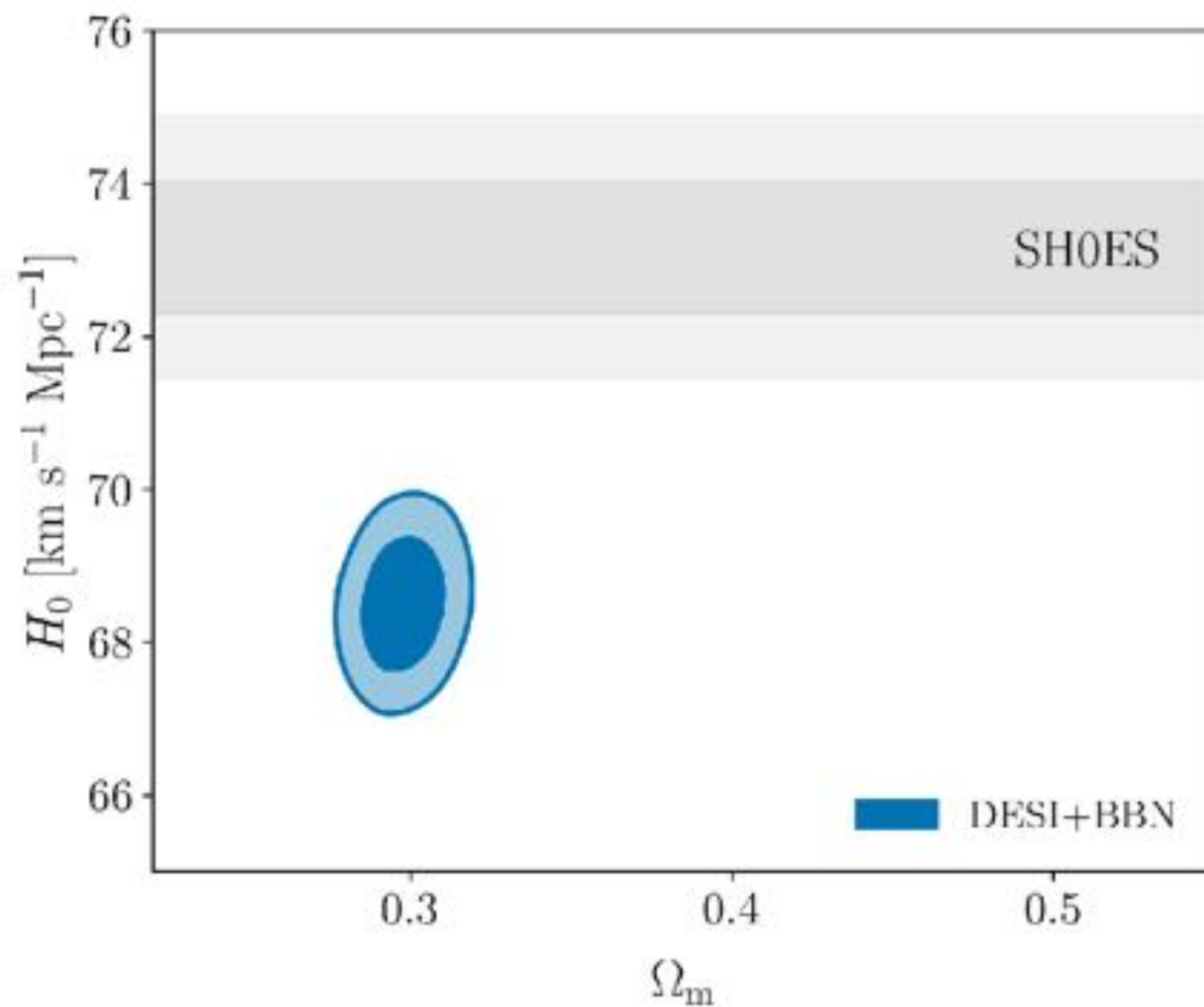
$$\left. \begin{aligned} \Omega_m &= 0.2975 \pm 0.0086, \\ hr_d &= (101.54 \pm 0.73) \text{ Mpc}, \end{aligned} \right\} \text{ DESI DR2.}$$



DARK ENERGY
SPECTROSCOPIC
INSTRUMENT

U.S. Department of Energy Office of Science

Constraints under Λ CDM



In Λ CDM, the tension between the **DESI+BBN** and SH0ES H_0 (Breuval++2024) now stands at 4.5σ , independent of the CMB.

II. Dark Energy beyond Λ CDM

For a cosmological constant, the dark energy **equation of state** is given by

$$w = \frac{p}{\rho c^2} = -1$$

The equations of motion are well approximated by
(Chevalier & Polarski 2001, Linder 2003)

$$w(a) = w_0 + w_a(1 - a)$$

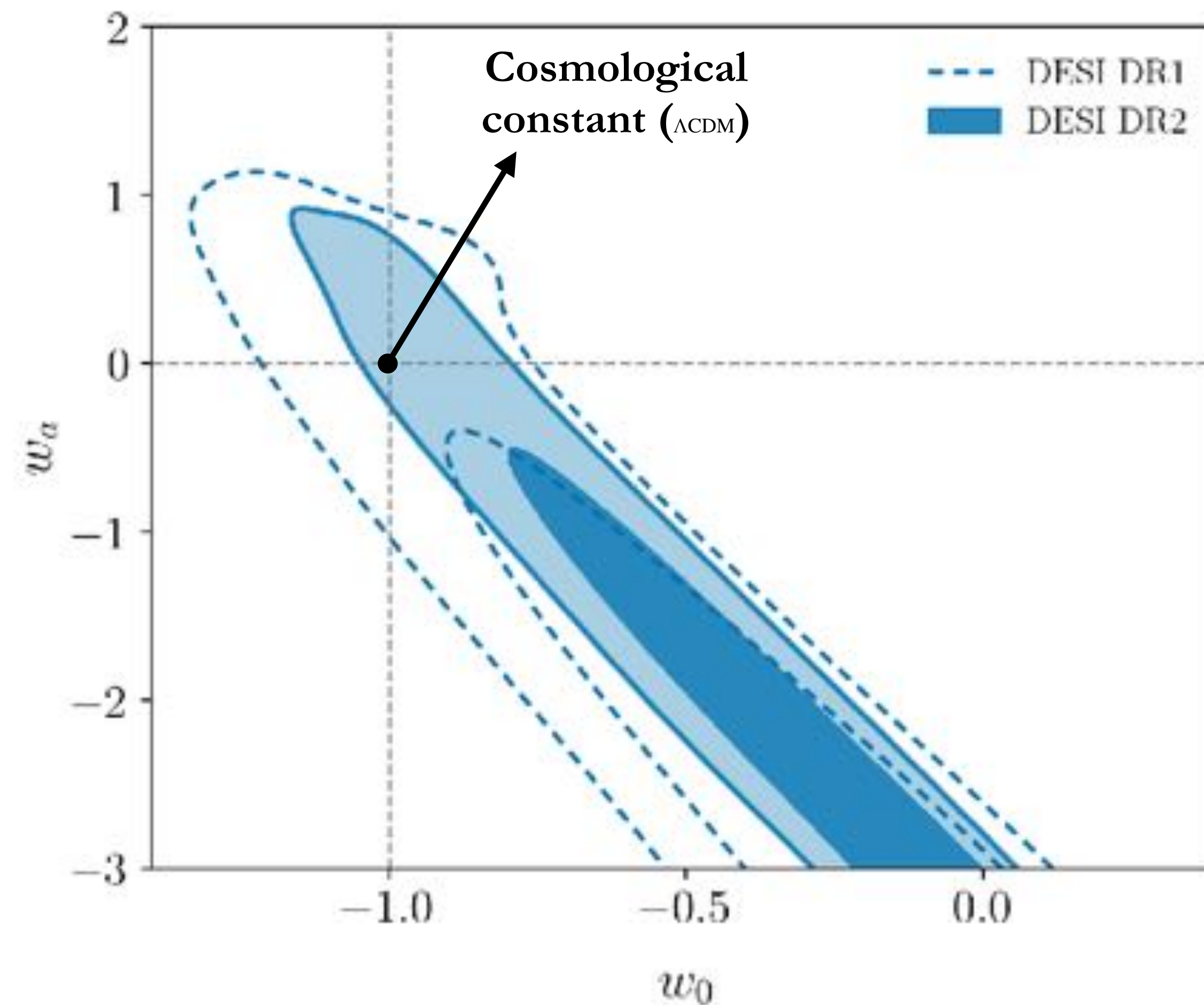


DARK ENERGY
SPECTROSCOPIC
INSTRUMENT

Dynamical Dark Energy

U.S. Department of Energy Office of Science

- BAO data define a degeneracy direction in the w_0 - w_a plane.
- BAO data by itself does not rule out the cosmological constant, but its combination with more data sets leads to tight constraints.





DARK ENERGY
SPECTROSCOPIC
INSTRUMENT

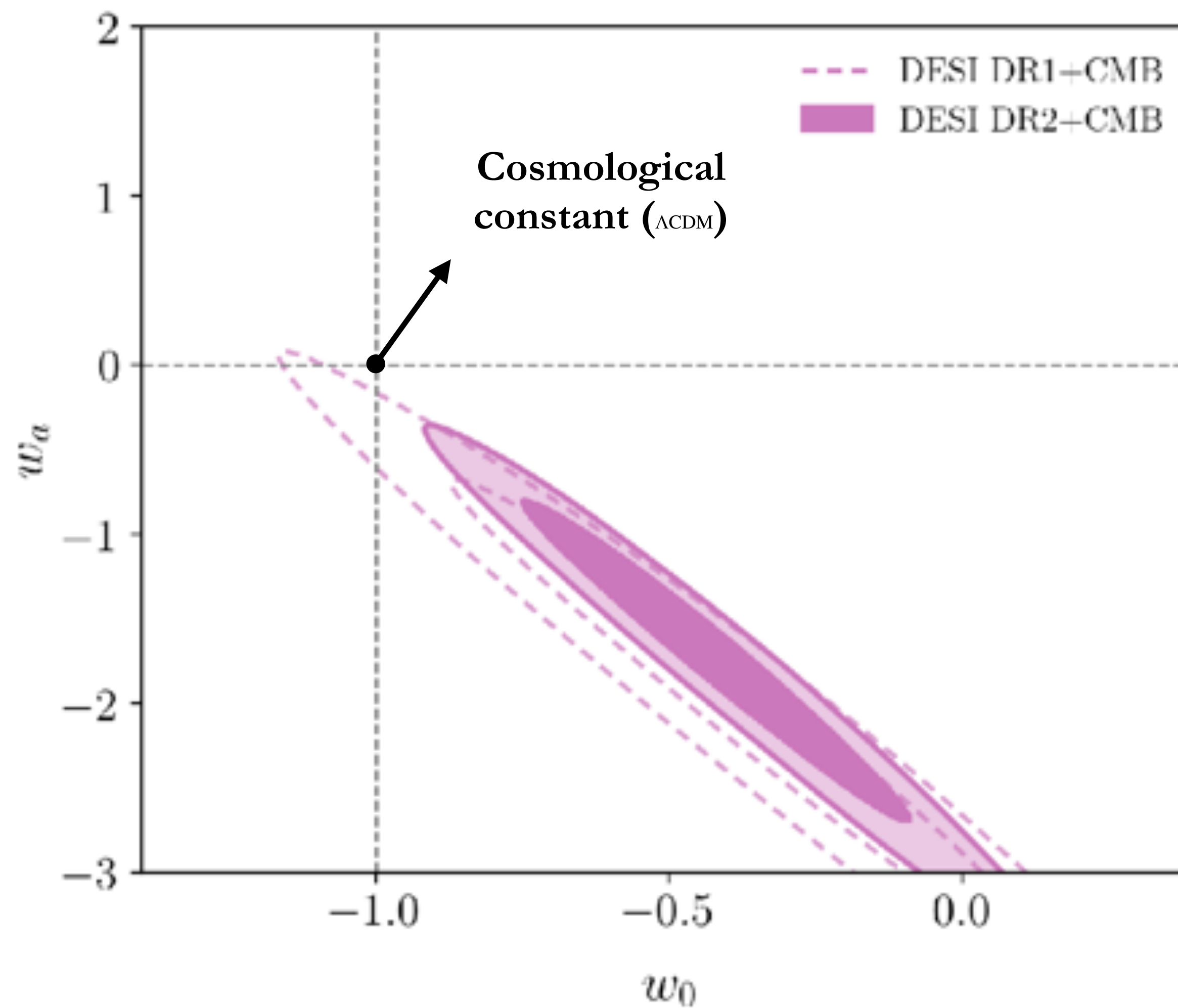
Dynamical Dark Energy

U.S. Department of Energy Office of Science

- Last year: 2.6σ preference for evolving dark energy from DESI BAO+CMB

—> 3.1σ in DR2

$$\left. \begin{aligned} w_0 &= -0.42 \pm 0.21 \\ w_a &= -1.75 \pm 0.58 \end{aligned} \right\} \text{DESI+CMB}$$



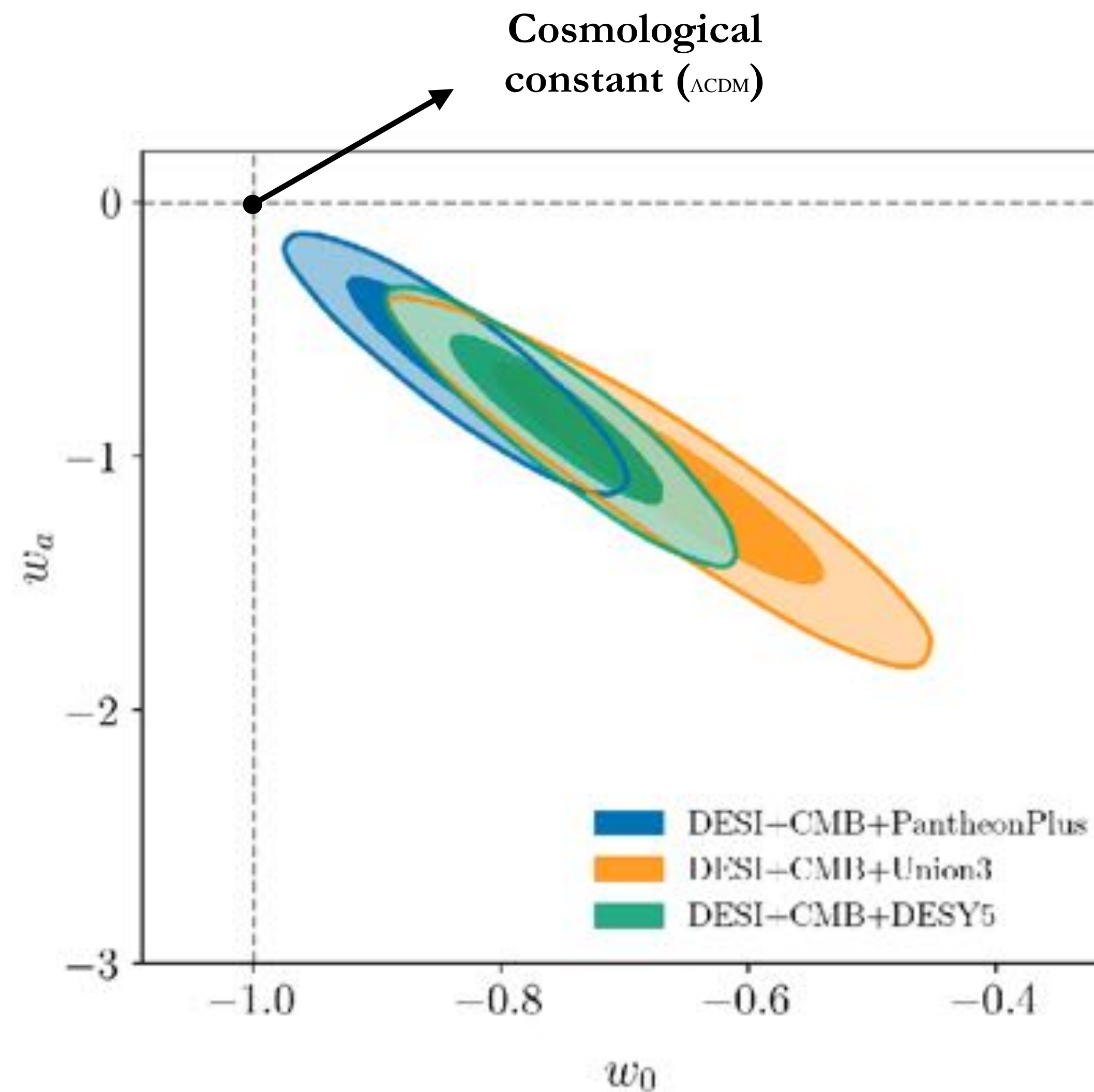


DARK ENERGY
SPECTROSCOPIC
INSTRUMENT

U.S. Department of Energy Office of Science

Dynamical Dark Energy

- Significance of rejection of Λ CDM:
 - DESI+CMB+Pantheon+: 2.8σ
 - DESI+CMB+Union3 : 3.8σ
 - DESI+CMB+DESY5: 4.2σ





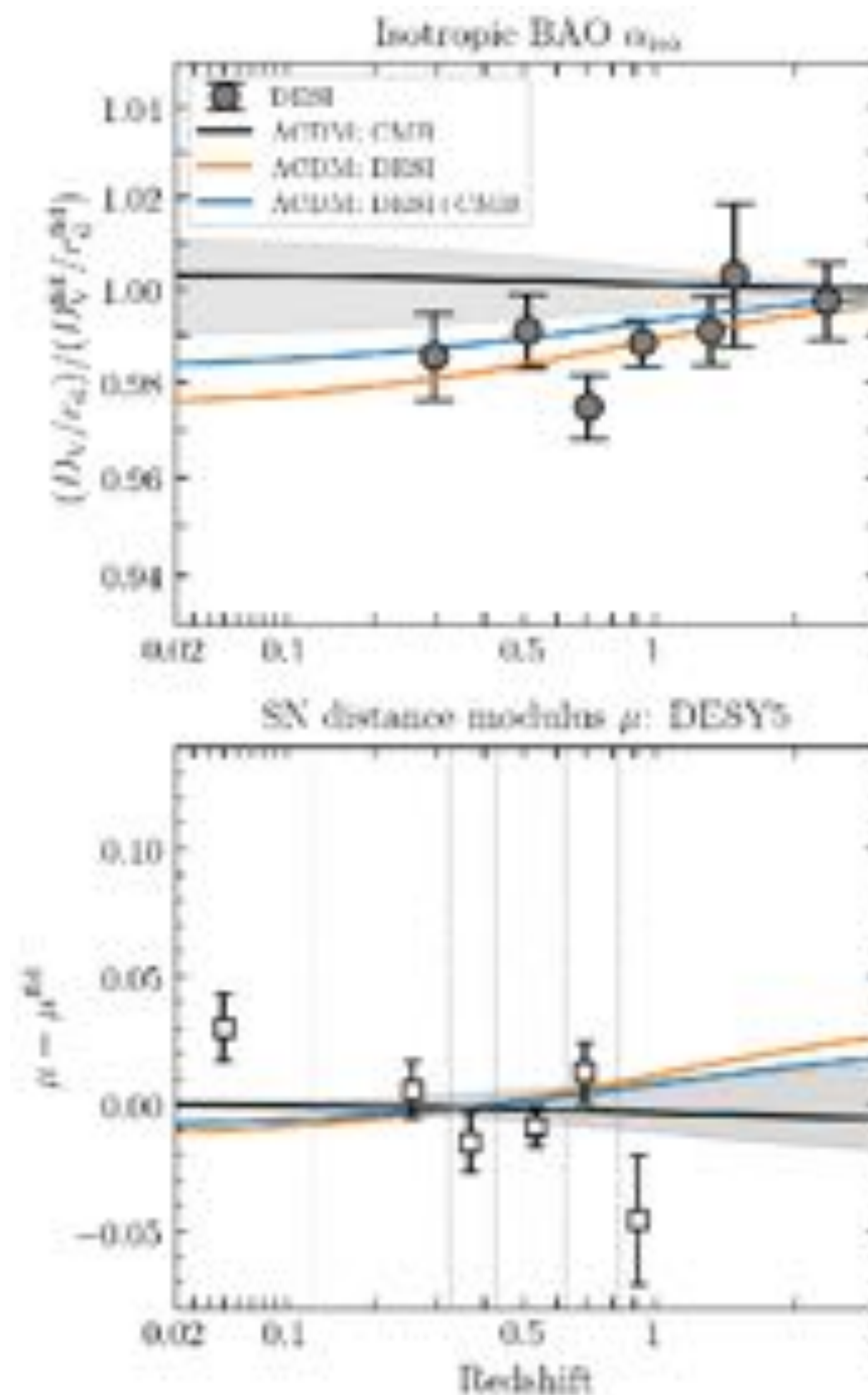
DARK ENERGY
SPECTROSCOPIC
INSTRUMENT

U.S. Department of Energy Office of Science

Dynamical Dark Energy

Isotropic BAO distance
measurement

Supernovae distance
modulus



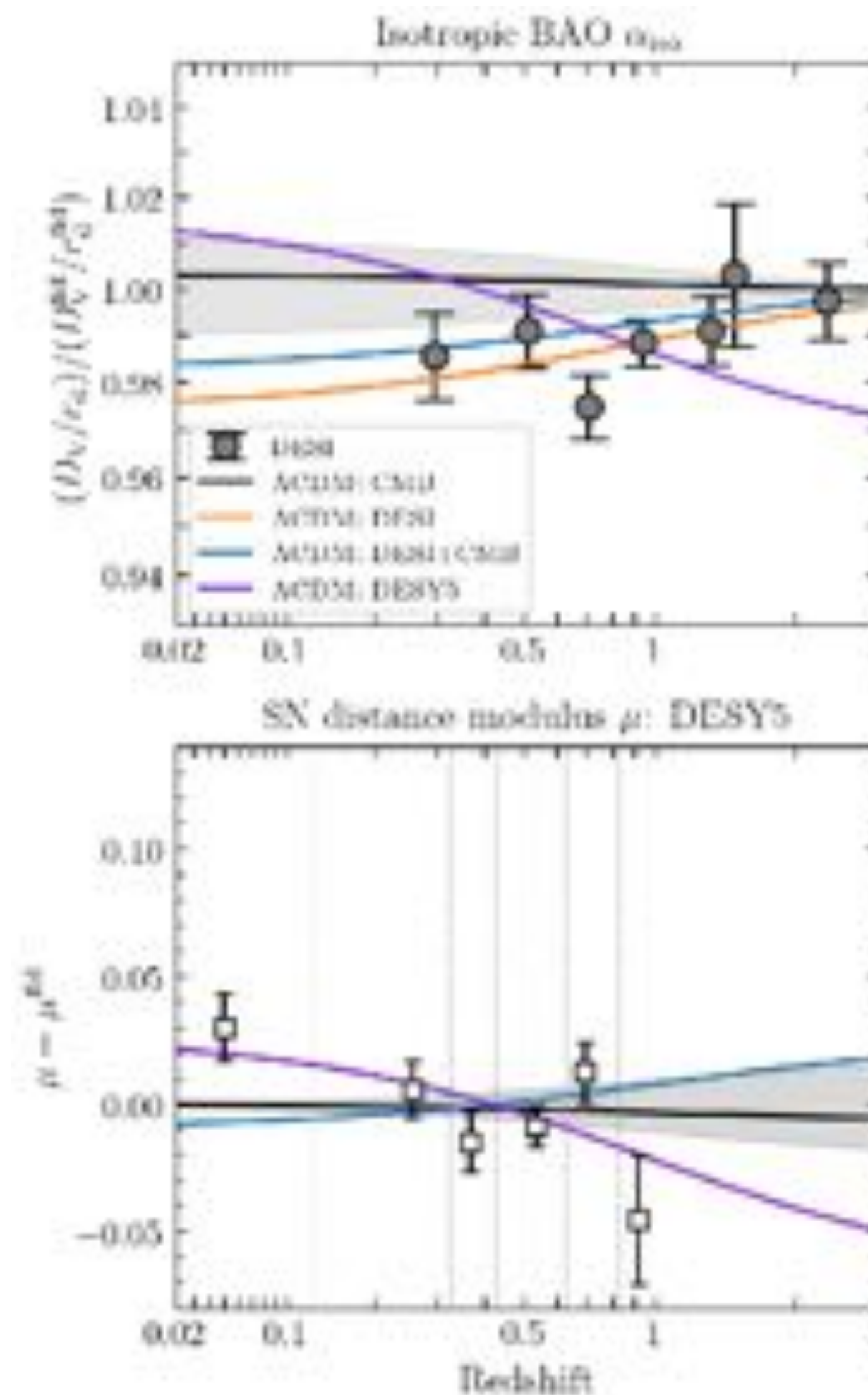
- There are Λ CDM models that each dataset prefer, but they are inconsistent in their Ω_m values.



DARK ENERGY
SPECTROSCOPIC
INSTRUMENT

U.S. Department of Energy Office of Science

Dynamical Dark Energy



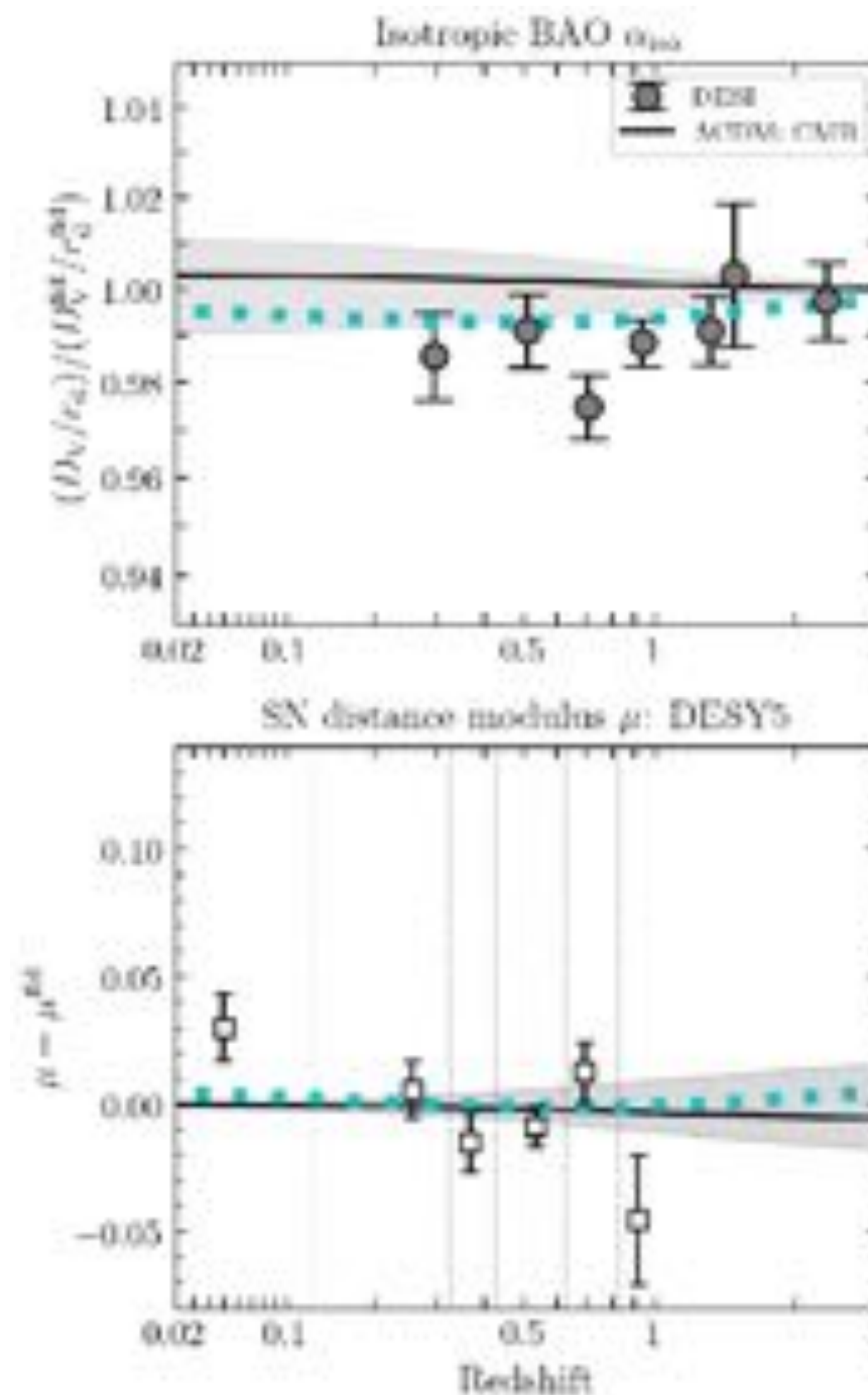
- There are Λ CDM models that each dataset prefer, but they are inconsistent in their Ω_m values.
- Λ CDM does not provide a good fit to all data simultaneously.



DARK ENERGY
SPECTROSCOPIC
INSTRUMENT

Dynamical Dark Energy

U.S. Department of Energy Office of Science



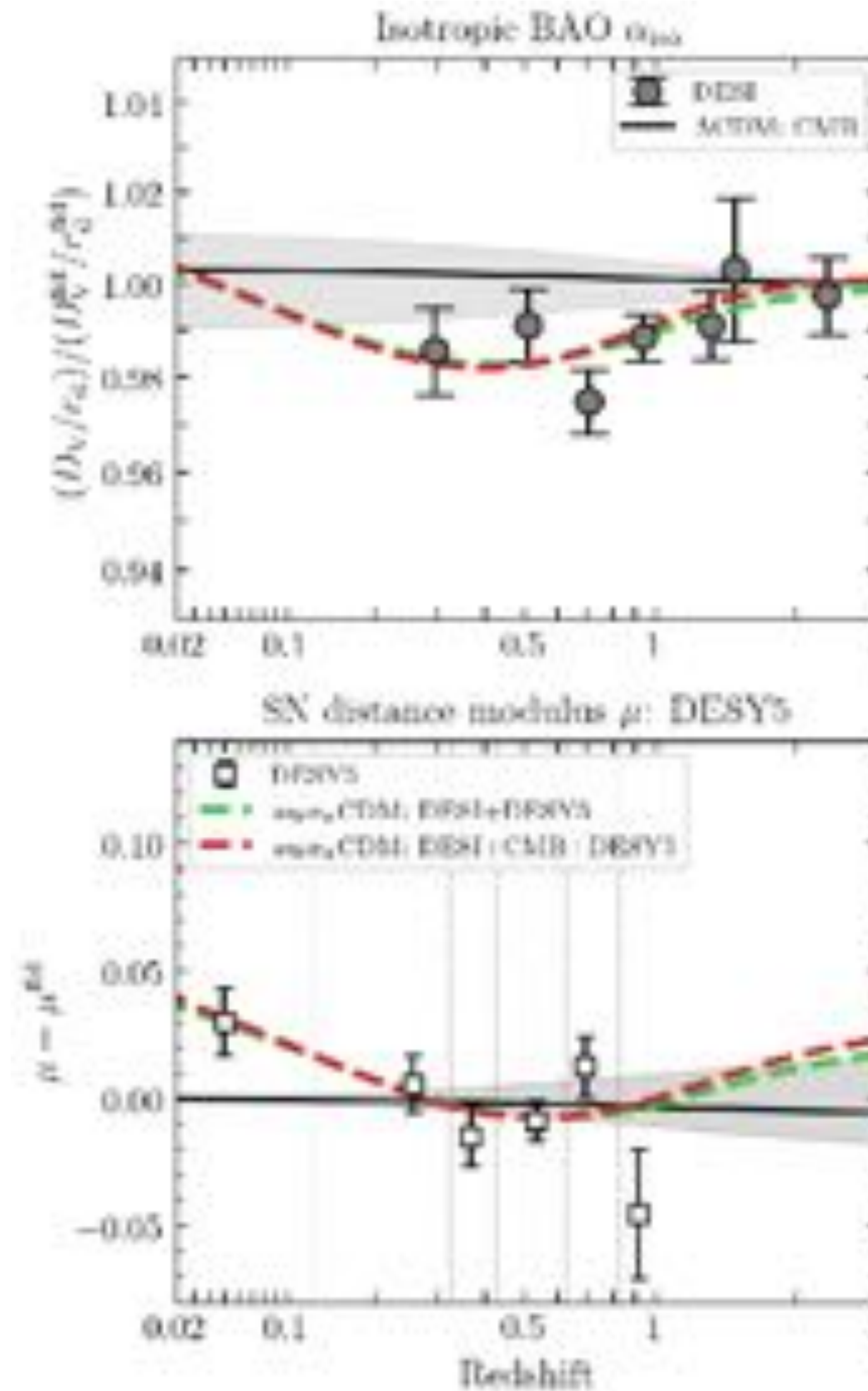
- w_{CDM} model: constant equation of state $p/(\rho c^2)$, but not necessarily equal to -1.
- w_{CDM} does not have enough freedom in the expansion history to fit BAO, CMB, and SNe simultaneously.



DARK ENERGY
SPECTROSCOPIC
INSTRUMENT

U.S. Department of Energy Office of Science

Dynamical Dark Energy



- w_0w_a CDM has sufficient flexibility to simultaneously achieve good fits to all three datasets.
- Resolves the mismatch in Ω_m between DESI and CMB.

Evolution of clustering in cosmological models with time-varying dark energy

Tomoaki Ishiyama*

Digital Transformation Enhancement Council, Chiba University,
1-33, Yayoi-cho, Inage-ku, Chiba, 263-8522, Japan

Francisco Prada

Instituto de Astrofísica de Andalucía (CSIC), Glorieta de la Astronomía, E-18080 Granada, Spain

Anatoly A. Klypin

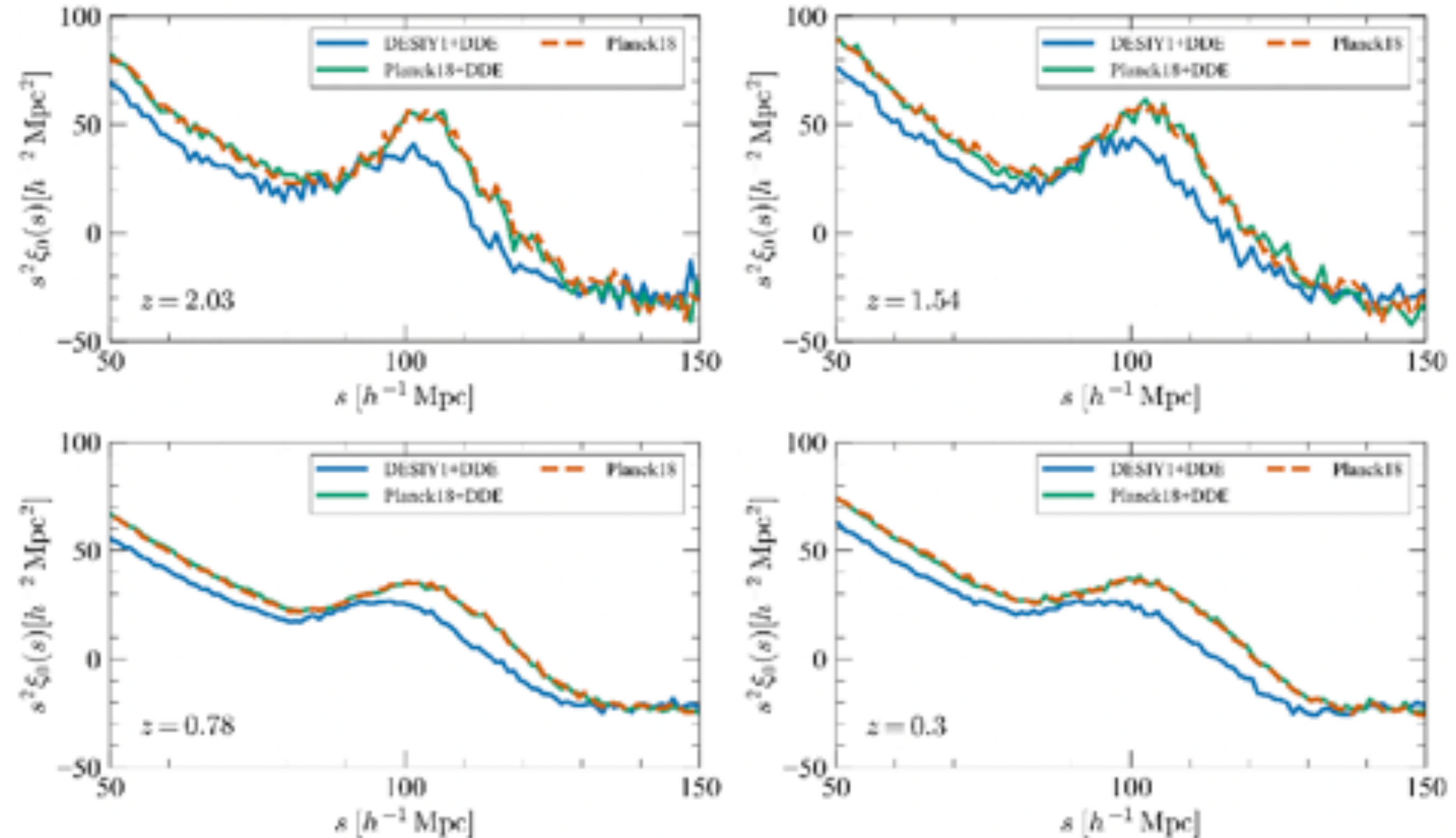
Astronomy Department, New Mexico State University, Las Cruces, NM, USA and
Department of Astronomy, University of Virginia, Charlottesville, VA, USA

(Dated: March 28, 2025)

Observations favor cosmological models with a time-varying dark energy component. But how does dynamical dark energy (DDE) influence the growth of structure in an expanding Universe? We investigate this question using high-resolution N -body simulations based on a DDE cosmology constrained by first-year DESI data (DESIY1+DDE), characterized by a 4% lower Hubble constant (H_0) and 10% higher matter density (Ω_0) than the Planck-2018 Λ CDM model. We examine the impact on the matter power spectrum, halo abundances, clustering, and Baryonic Acoustic Oscillations (BAO). We find that DESIY1+DDE exhibits a 10% excess in power at small scales and a 15% suppression at large scales, driven primarily by its higher Ω_0 . This trend is reflected in the halo mass function: DESIY1+DDE predicts up to 70% more massive halos at $z = 2$ and a 40% excess at $z = 0.3$. Clustering analysis reveals a 3.71% shift of the BAO peak towards smaller scales in DESIY1+DDE, consistent with its reduced sound horizon compared to Planck18. Measurements of the BAO dilation parameter α , using halo samples with DESI-like tracer number densities across $0 < z < 1.5$, agree with the expected DESIY1+DDE-to-Planck18 sound horizon ratio. After accounting for cosmology-dependent distances, the simulation-based observational dilation parameter closely matches DESI Y1 data. We find that the impact of DDE is severely limited by current observational constraints, which strongly favor cosmological models – whether including DDE or not – with a tightly constrained parameter $\Omega_0 h^2 \approx 0.143$, within 1-2% uncertainty. Indeed, our results demonstrate that variations in cosmological parameters, particularly Ω_0 , have a greater influence on structure formation than the DDE component alone.

arXiv:2503.19352

| Parameter | Planck18 | Planck18+DDE | DESIY1+DDE |
|-----------------------|----------|--------------|------------|
| Ω_0 | 0.3111 | 0.3111 | 0.3440 |
| h | 0.6766 | 0.6766 | 0.6470 |
| w_0 | -1.0 | -0.45 | -0.45 |
| w_a | 0.0 | -1.79 | -1.79 |
| z_d | 1060.02 | 1060.02 | 1055.70 |
| r_d [h^{-1} Mpc] | 99.61 | 99.61 | 96.05 |



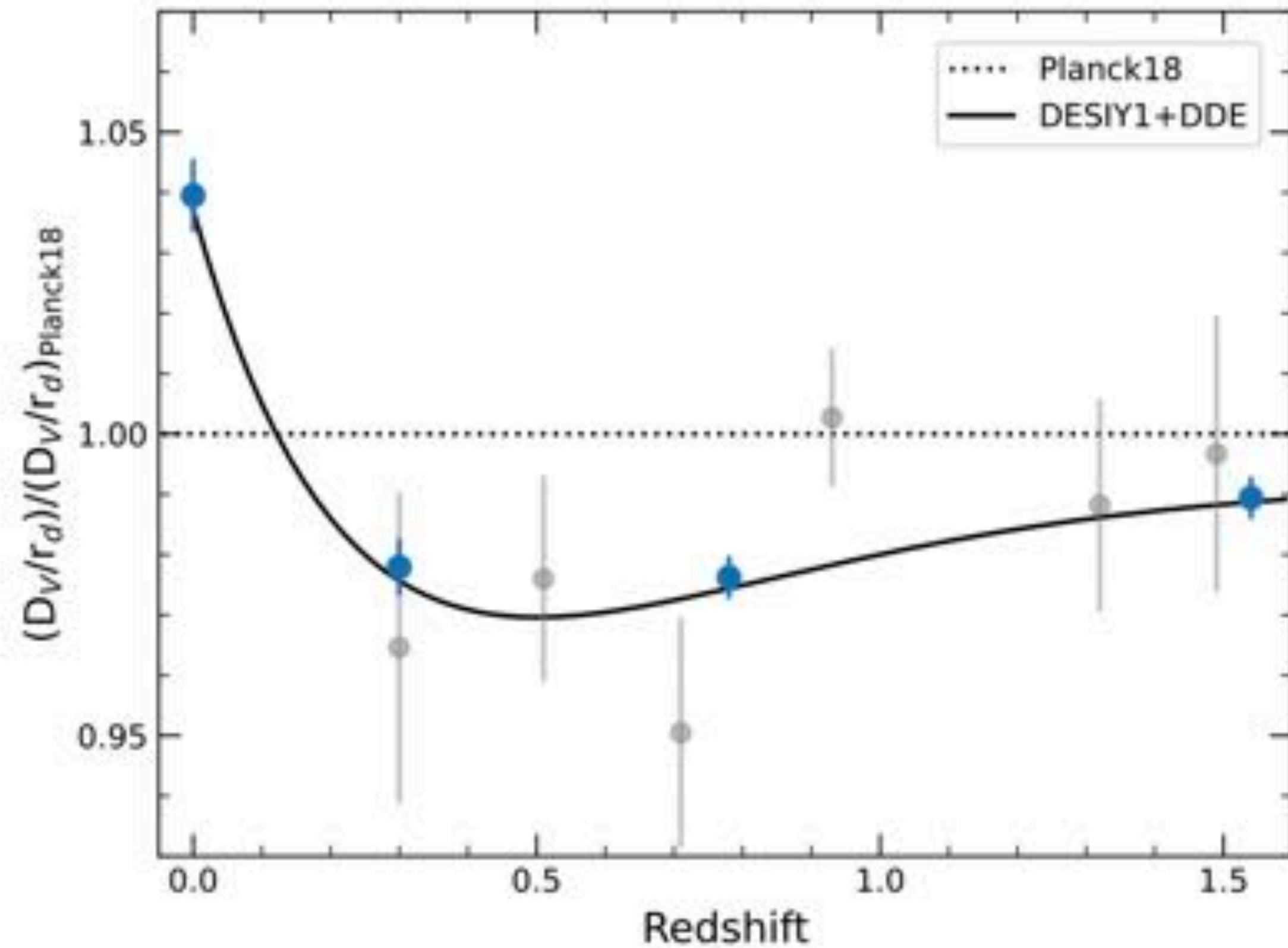


FIG. 6. Acoustic-scale distance measurements relative to the prediction from the Planck18 model. The gray symbols with 1σ error bars represent the isotropic BAO measurements, $D_V(z)/r_d$, from DESIY1 [1], shown in order of increasing redshift. The curve shows the model prediction from the DESIY1+DDE cosmology, which closely matches the BAO distance measurements (blue symbols) obtained from the halo samples in our DESIY1+DDE simulation, as listed in Table II.

- We find that for all statistics we studied – the matter power spectrum, halo mass function, and halo clustering – the impact of the DDE alone is smaller than the effect of the differences in cosmological parameters between Planck18 and DESIY1.
- Current observations favor cosmological models with nearly the same value of the product $\Omega_0 h^2$ [2]. Estimates based on both plain Λ CDM and DDE models consistently fall within a narrow $\sim 1 - 2\%$ range around $\Omega_0 h^2 = 0.143$.
- The halo mass function reflects these trends, with DESIY1+DDE predicting up to 70% more massive halos at $z = 2$, and sustaining a 40% excess at $z = 0.3$.
- Clustering analysis reveals a 3.71% shift of the BAO peak towards smaller scales in the DESIY1+DDE model, resulting from the reduced sound horizon scale compared to Planck18. Measurements of the α dilation parameter, using halo samples with DESI-like tracer number densities across redshifts $0 < z < 1.5$, yield values consistent with the DESIY1+DDE-to-Planck18 sound horizon ratio. After accounting for cosmology-dependent distances, the simulation-based observational dilation parameter closely matches DESI Y1 observations.



DARK ENERGY
SPECTROSCOPIC
INSTRUMENT

U.S. Department of Energy Office of Science

DESI instrument

Mayall telescope
at Kitt Peak Observatory (AZ)



Nathalie Palanque-Delabrouille (LBNL)



**DARK ENERGY
SPECTROSCOPIC
INSTRUMENT**

U.S. Department of Energy Office of Science

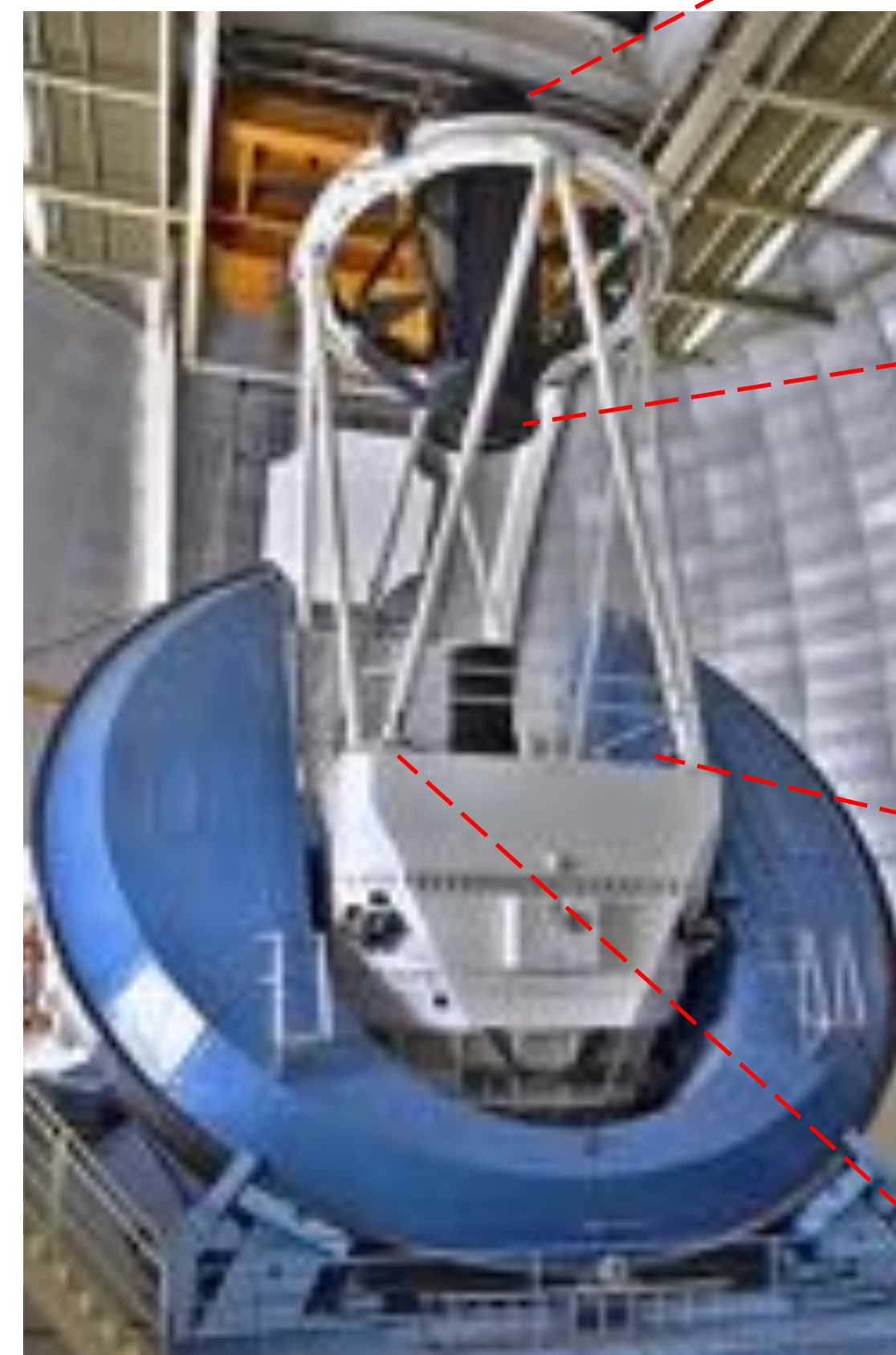
DESI instrument

40m-long
optical fibers



**5000 optical fiber
robot positioners**

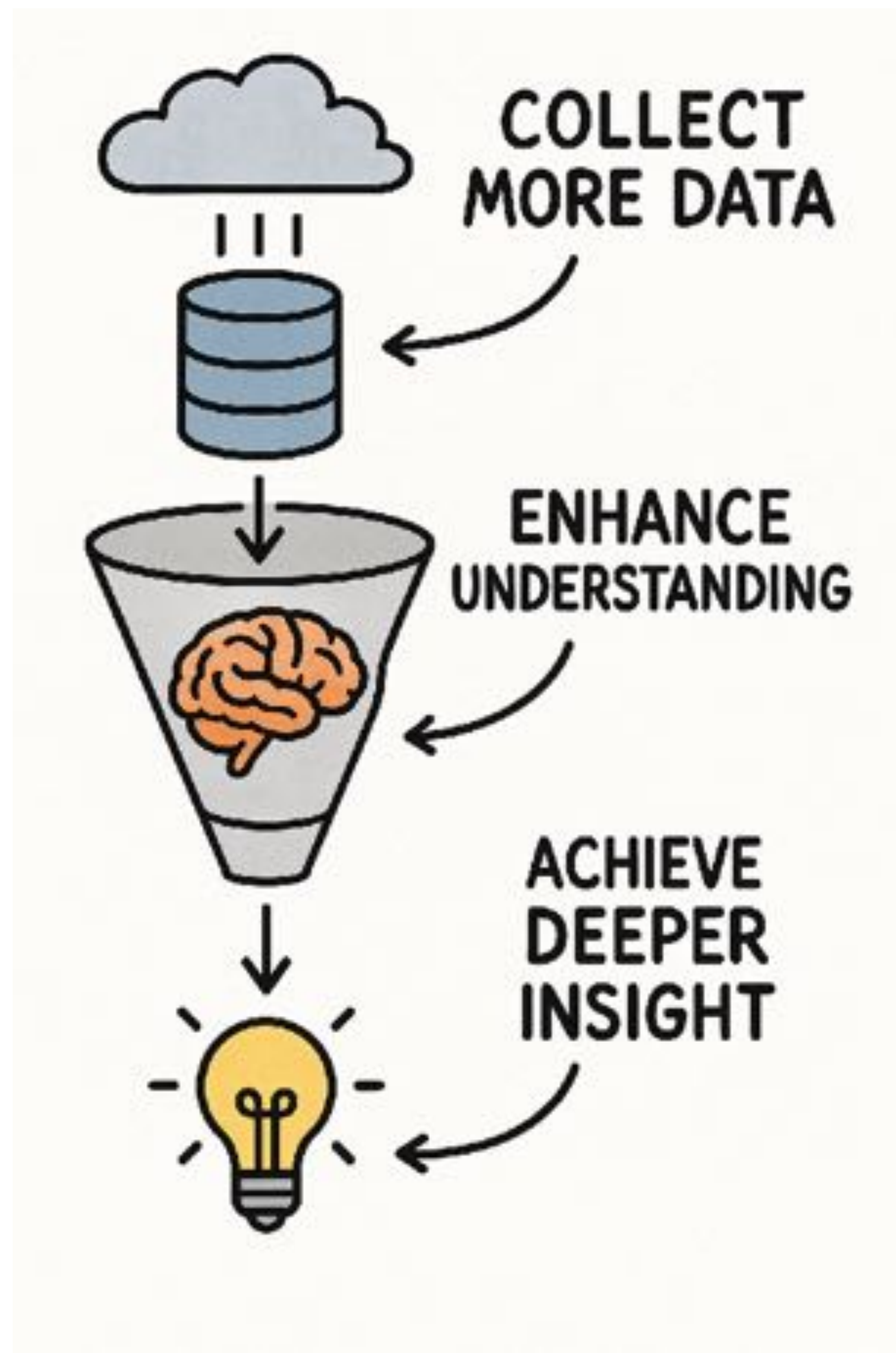
10 3-band spectrographs



**7 deg²
field of view**

**4m mirror
(large collecting area)**





conclusions